

Elucidating the mode of action of  
Occidiofungin – a current first in class  
antifungal

Louis Harger

Microbiology MSc-R 2025

School of Biosciences

Word Count (12,146)

## Abstract

Fungal infections are responsible for an approximate 1.5 million deaths annually, with there being no licensed vaccines or vaccines currently in clinical study for fungal disease. This combined with the increasing resistance to the current antifungals in clinical use, highlights an ever increasing need for new antifungal research. My research aims to elucidate the mode of action of a current first in class antifungal known as Occidiofungin. This antifungal is currently undergoing clinical trials and has shown potent broad spectrum activity in the treatment of pathogenic yeast. My aim was to determine the mechanism that this drug uses in order to kill fungal cells. Previous research suggested that Occidiofungin may target the Actin cytoskeleton and as Actin is essential to cell function this may represent a plausible mode of action. I employed a range of techniques to investigate whether Occidiofungin inhibits the function of Actin and whether recognised Actin-related modes of cell death were activated. My findings suggest that Actin is not targeted but rather Occidiofungin induces necrosis in cells in a gradual manner. This finding was strengthened by observations that a fluorescent tagged Occidiofungin (Alkyne Occidiofungin) was not internalised but accumulated at the outer surface of the yeast cell. The fungal specificity of Occidiofungin was also investigated through the use of haemolysis assays and the *Galleria mellonella* infection model. This pre-clinical data suggested that Occidiofungin is indeed fungal specific and so is a promising candidate for use as a future therapeutic. Future research will determine the fungal specific target of Occidiofungin that is responsible for the induction of necrosis which may in turn lead to the expansion of this class of antifungal. If targeting the fungal cell wall, upon recognition of the target component, this would have broad applications both in the knowledge of the drug and proof that it has fungal specificity, it could also indicate a novel site that could be used in drug design and development.

## Acknowledgements

I would firstly like to say a huge thank you to Dr. Campbell Gourlay, for giving me the opportunity to start this exciting research, as well as all the ideas and advice that he gave to me along the way which have vastly improved my lab technique and understanding. I would also like to thank Sano Chemicals for supplying me with the Occidiofungin and Alkyne Occidiofungin to use in my experimentations, as well as discovering this remarkable drug which spawned the whole premise of my research masters.

I would also like to give a big thank you to the members in the Gourlay lab for their very generous help and support not just in my research but outside of it too. With special thanks to Ed, Jack, Sammy and Dima for lending a helping hand in different experiments.

I would also like to thank family for the support they have given me, whom without them I may have been less inclined to start my Masters so soon.

## **Declaration**

No part of this thesis has been submitted in support of an application for any degree or qualification of the University of Kent or any other University or Institute of Learning.

Louis Harger

# Contents

Abstract .....	2
Acknowledgements .....	3
Declaration .....	4
Contents .....	5
List of figures .....	8
1 Introduction .....	16
1.1 Current burden of fungal disease .....	16
1.2 <i>Candida</i> infection .....	17
1.3 Occidiofungin - a novel first in class antifungal .....	25
1.4 Actin as a potential target of Occidiofungin .....	26
1.5 Cofilin .....	32
1.6 Aims of my research.....	33
2. Materials and Methods .....	34
2.1 Yeast strains and Growth .....	34
2.2 Minimum Inhibitory Concentration (MIC) Assay .....	37
2.3 Assessment of ROS accumulation and Necrosis using Flow Cytometry .....	37
2.4 Analysis of lipid droplet number by fluorescence microscopy .....	38
2.5 Alkyne Occidiofungin imaging .....	39
2.6 Yeast plasmid transformation .....	39
2.7 Haemolysis Assay .....	41

2.8 <i>Galleria mellonella</i> infection and toxicity assay .....	42
2.9 Macrophage engulfment assay .....	43
2.10 <i>Candida albicans</i> Biofilm Assay .....	44
3 Results .....	46
3.1 Occidiofungin MIC <sub>50</sub> determination in <i>Saccharomyces cerevisiae</i> cells .....	46
3.1.1 ROS accumulation and necrosis in $\Delta por1$ cells when compared to Wild Type <i>Saccharomyces cerevisiae</i> using flow cytometry .....	47
3.1.2 Necrosis Assay to determine the death time course of <i>S.cerevisiae</i> cells upon Occidiofungin treatment .....	53
3.1.3 Use of Fluorescence microscopy to examine the effects of Occidiofungin treatment on lipid droplet formation in wild type and $\Delta por1$ cells .....	54
3.2 Ascertaining whether Actin is a target of Occidiofungin .....	56
3.2.1 Analysing a library of Actin mutant strains to assess a synthetic interaction with Occidiofungin .....	56
3.2.2 Using GFP tagged ABP-1 to assess the effect Occidiofungin has cortical Actin patch dynamics using fluorescence microscopy .....	60
3.3 Haemolysis assay to assess whether Occidiofungin treatment leads to Red Blood Cell lysis.....	61
3.3.1 Use of <i>Galleria mellonella</i> as an infection model to assess the efficacy and toxicity of Occidiofungin within a living system .....	62
3.3.2 Effects of Occidiofungin Treatment on Macrophage uptake of <i>C. albicans</i> cells.....	65

3.3.3 Assessment of the effects of Occidiofungin treatment on <i>C. albicans</i> biofilm formation.....	66
3.4 Testing Occidiofungin against a variety <i>Candida</i> species .....	68
3.5 Using an Alkyne derivatised Occidiofungin to examine Occidiofungin localisation.....	69
4. Discussion .....	70
4.1 Actin as a target for Occidiofungin .....	70
4.2. Occidiofungin effects on lipid storage .....	75
4.3 Occidiofungin is a promising anti-fungal .....	75
Conclusion .....	79
References .....	80

## List of Figures

- Figure 1.1.** Image to display the three morphological forms of *Candida albicans*. 1 - Yeast, small round cells that divide by conventional cell division. 2- Pseudohyphae less elongated hyphae, more constricted at septa compared to true hyphae. 3 - True hyphae, elongated cells that do not separate following cell division, separated by specialised septa that allow passage of cytoplasm and other components between compartments (11) ..... 18
- Figure 1.2.** Illustration to show mixed *C.albicans* and *Staphylococcus* species biofilm within a host environment. Molecular interactions between the two species are represented in: A - invasive endothelial infection with increased antimicrobial drug tolerance. B - altered infection outcome. C - as a result (12) ..... 19
- Figure 1.3.** Image of Conserved stress regulator pathways in *Candida albicans*. MAPK signalling molecules (red), transcription factors (blue), contribute to stress function regulations in *Candida albicans*. Hsf1/Hsp90 form autoregulatory circuit. Heat shock pathway: Hsp90, Hsf1, Nitrosative stress pathway: Cta4, Thb1. Cell integrity Pathway: Bck1, Mkk1, Mkc1. Oxidative stress pathway: Cap1, Skn7, SODs. Hog1 signalling pathway: Ssk2, Pbs2, Hog1 (23)..... 23
- Figure 1.4.** Diagram to compare stages of biofilm formation, in *Candida albicans*, *Candida glabrata*, *Candida tropicalis* and *Candida parapsilosis*. Highlighting the ability for these strains to produce an extracellular matrix, the various components that reside in the matrix as well as their ability to show different cell morphologies (32)..... 24
- Figure 1.5.** Diagram to show the structure of Occidiofungin A (left hand side) and Occidiofungin B (Right hand side) (33)..... 26

**Figure 1.6** Diagram to show a model of Endocytosis and Actin patch assembly. Phase I - indicates where most Arp2/3 regulators will promote the assembly to establish an Actin network with suitable filament lengths and branch density. Phase II - The Arp2/3 regulation complex, there are no single regulator mutation affects this stage, but mutations in WASp/Las17, Myo3 and in Myo5 disrupt movement. Phase III - Actin filaments that were nucleated at the Actin patch, drive vesicle movement in the cytoplasm

(36)..... 27

**Figure 1.7** Diagram to VDAC-dependant MAPK signalling. In Wild type cells the Actin cytoskeleton is polarised along the mother-bud axis, a cell wall stress then depolarises the cytoskeleton, this triggers the Cell wall integrity MAPK pathway, leading to transcriptional adaptation of cell wall genes, promoting cell survival. In *cof1-5* cells Actin is stabilised and chronically depolarised, constantly triggering the Cell wall integrity pathway, Pkc1 and Slt2 localize to the mitochondrion (Por1 dependant), this causes loss of lipid homeostasis, lipid droplet accumulation, vacuole fragmentation and cell wall defects

(43)..... 30

**Figure 1.8.** Image to show Effects of Occidiofungin exposure on the integrity of Actin cables in *S. cerevisiae* cells. A represents the DMSO control, Actin patches and cables are visible from arrows. B represents Occidiofungin treatment at 0.5x the MIC for 30 minutes, cables are lost and Actin aggregates accumulate, scale bars represent 2µm (44) ..... 32

**Table 2.1.** Table containing all the Yeast strains used in experimentation over the course of the project. *Act1* Mutants (45). *Candida albicans* - *SN250* (46)..... 35

**Figure. 3.1** Growth curve to show *Saccharomyces cerevisiae* cells treated with varying concentrations of Occidiofungin. Occidiofungin was serially diluted along columns 2-9, with each step representing a 2-fold dilution. This resulted in a final dilution of 128-fold in the last

column. Starting concentration was  $3.2 \mu\text{g mL}^{-1}$ , columns 10 and 11 were used as controls, with a YPD control and an untreated control. Cells were grown overnight at  $30^\circ\text{C}$  in YPD, diluted and then added to the wells at a final OD of 0.1. The plates were then placed in a SpectroStarNano and grown for 24 hours at  $30^\circ\text{C}$ . The results were then used to make a line graph which was then placed into GraphPad for analysis of area under the curve and this was plotted on the X-axis and the Log of each Occidiofungin concentration on the Y-axis. The graph represents a single representative

experiment..... 47

**Figure 3.2.** Cell type classification in conjunction with H2DCF-DA and PI signal characteristics.

A positive control group of untreated cells were grown to log phase in YPD media without addition of PI. Cells below the y-axis threshold were classified as Low ROS, whilst those that breached the x-axis threshold were perceived as necrotic. Live cells (non-necrotic) are measured through the proportion of cells occupying the lower quadrants. Each Quadrant

condition is labelled above. A - Wt. B - *Δpor1*. ..... 49

**Figure 3.3.** Plots to show the heat treated positive controls of both cell types, this shows the profile of fully necrotic cells that were heated to  $100^\circ\text{C}$  for 15 minutes. These samples were then ran through the flow cytometer to give the graph profiling seen above. A - Wt. B -

*Δpor1*..... 49

**Figure 3.4.** Graphs to display the cell classifications after 60 minutes treatment of

Occidiofungin at a concentration of  $0.24 \mu\text{g mL}^{-1}$  in both Wt and *Δpor1* *S.cerevisiae* cells. Cells were grown overnight and then diluted to an OD of 0.1, these cells were then grown to log phase, after they reached log phase Occidiofungin was added and they were treated for 60 minutes at  $30^\circ\text{C}$ . The cells were then run through the flow cytometer. These graphs are used

as a representative for 3 biological replicates that were conducted for these controls. A - Wt. B - *Δpor1* ..... 50

**Figure 3.5.** Bar graph displaying the Quadrant percentages shown through the PI/H2DCF-DA staining results for *Δpor1* and Wt cells treated with 0.24μgmL<sup>-1</sup> Occidiofungin. Each Condition represents the average from 3 biological repeats. The error bars represent the standard deviation between the biological repeats. The statistical significance was tested using t-Test: Two-Sample Assuming Equal Variance data analysis tool in excel. Statistical significance is represented via the bars with asterixis, these bars represent quadrants that are significantly different from each other (P value < 0.05) ..... 51

**Table 3.1.** Table to show the P-value from t-Test: Two-Sample Assuming Equal Variance that was carried out on select controls. This was to assess whether there was a significant difference in the percentages of each separate quadrant. It also analysed whether the quadrant values of the Wt and *Δpor1* cells were significantly different under treatment of Occidiofungin. P<0.05..... 52

**Figure 3.6.** Graph to show the necrosis of Log phase *S.cerevisiae* cells treated with 0.35μgmL<sup>-1</sup> Occidiofungin compared with cells that remained untreated at 30°C. PI was added at 10 μg/mL prior to running samples through a flow cytometer at 15 minute intervals to show the percentage of cells necrotised at each timepoint, over a 2 hour treatment period. This graph is a single representative experiment, with no technical replicates..... 53

**Figure 3.7.** Image to show lipid droplets (white dots) present in Wt *S.cerevisiae* cells grown to log phase and then treated with 0.24μgmL<sup>-1</sup> Occidiofungin for a 2 hour time period. Displaying the effects of the treatment in 1 hour increments. Cells were stained with Bodipy 493/503. Images were gathered using an Olympus IX81 fluorescence microscope, with GFP 395/509

nm excitation/emission, at 100x magnification, using an Andor Xyla 4.2 CMOS digital camera..... 54

**Figure 3.8.** Image to show lipid droplets (white dots) present in  $\Delta por1$  *S.cerevisiae* cells grown to log phase and then treated with  $0.24\mu\text{g mL}^{-1}$  Occidiofungin for a 2 hour time period.

Displaying the effects of the treatment in 1 hour increments. Cells were stained with Bodipy 493/503. Images were gathered using an Olympus IX81 fluorescence microscope, with GFP 395/509 nm excitation/emission, at 100x magnification, using an Andor Xyla 4.2 CMOS digital camera..... 55

**Table 3.2.** Table to show the average lipid droplet count per cell in both the Wt and  $\Delta por1$  cells, each average was taken from a minimum of 18 cells and are representative of the two Figures 3.8 and 3.7 as a single experimentation without repeats. The percentage difference between the lipid droplet counts of the two cell types was calculated and displayed above..... 55

**Figure 3.9.** Graph to show the normal growth of the *S.cerevisiae* Wt and different Actin mutant strains, at  $37^{\circ}\text{C}$  in a 24 hour time period. A SpectroStarNano Plate reader was used to record this. Each point on the graph represents an average from 3 technical replicates..... 57

**Figure 3.10.** Graph to show growth *S.cerevisiae* Wt and different Actin mutant strains when treated with  $0.35\mu\text{g mL}^{-1}$  Occidiofungin at  $37^{\circ}\text{C}$  in a 24 hour period. A SpectroStarNano Plate reader was used to record this. Each point on the graph represents an average from 3 technical replicates..... 57

**Figure 3.11.** Bar graph to show the area under the curve from the untreated and treated Actin mutants. This graph was made using the two figures above. The error bars are representative of the standard deviation between 3 technical replicates at each control. The statistical test carried out was a 1 tail Paired distribution t-test, this was carried out using the 3 technical replicates at

each control. Statistical significance is represented via the bars with asterixis, these bars represent quadrants that are significantly different from each other. P-value < 0.05..... 58

**Table 3.3.** Table to show the area under the curve for each mutant strain in the treated and untreated assays in a 24 hour period. This table is representative of Figure 3.11. This table shows the Statistical significance of the different strains when the Occidiofungin treated controls are compared to the untreated controls. This was done using the average of 3 technical repeats for the area under the curve. The statistical test carried out was a 1 tail Paired distribution t-test, this was carried out using the 3 technical replicates at each control. P<0.05..... 59

**Figure 3.12. A** - displays 3 kymographs that are representative of 3 different loci to on an untreated *Saccharomyces cerevisiae* cell, they represent the time taken for an Actin patch to endocytose within the cell and subsequently disappear from view under the microscope. These were taken from a 2 minute timelapse using a widefield microscope. **B** - displays kymographs for *Saccharomyces cerevisiae* cells that have been treated for 90 minutes with  $0.35\mu\text{g mL}^{-1}$  Occidiofungin. These were taken from a 2 minute timelapse using the widefield microscope. **C** - displays a bar graph with the average time taken for an Actin patch to endocytose from the membrane of the *Saccharomyces cerevisiae* cell, with the error bars representative of the Standard deviation between each replicate. The x-axis shows the control that each bar represents. **D** - Image displaying the GFP-ABP1 Actin cortical patches in an *S.cerevisiae* cell that has not been treated with Occidiofungin. **E**- Image displaying the GFP-ABP1 Actin cortical patches in an *S.cerevisiae* cell that had been treated for 90 minutes with  $0.35\mu\text{g mL}^{-1}$  Occidiofungin. These values were calculated using a velocity measurement tool in ImageJ. The Kymographs were made using ImageJ ..... 60

**Figure 3.13.** Picture of a blood agar plate after a 24 hour incubation at 37°C, 10% SDS used as a positive lysis control. H<sub>2</sub>O was used as a negative control. The other four differing concentrations represent Occidiofungin. This was repeated on 4 identical plates, with each

result displaying the same phenotype (Only the 10% SDS positive control led to the ring formation seen around the middle filter paper disc). This plate was representative for all repeats ..... 61

**Figure 3.14.** Graph to show *Galleria mellonella* survivability assay over a 7 day period, testing the toxicity of  $35\mu\text{g mL}^{-1}$  Occidiofungin using 3 other controls, 1.1% DMSO, PBS and a Non injection control. Each larvae were kept at  $37^{\circ}\text{C}$  for the duration of the 7 days. Each worm was injected into their bottom left proleg, as well as selected at similar size and phenotype..... 63

**Figure 3.15.** Survivability graph to display the survivability of 5 different *Galleria mellonella* controls. Each control contained 15 wax larvae; they were kept in an incubator at  $37^{\circ}\text{C}$  for the duration of the 7 day assay. All controls containing Occidiofungin used a concentration of  $1.6\mu\text{g mL}^{-1}$ . *Candida* PT - *Candida* that was pre-treated for 2 hours with Occidiofungin before it was injected into the larvae. *Candida* + Occidiofungin OP - *Candida albicans* and Occidiofungin were both injected but into separate pro legs ..... 64

**Figure 3.16.** Bar graph to show the average percentage of the total number of cells that were up took by the macrophages in the macrophage engulfment assay. These values were calculated using 4 images at each control, with the cell numbers counted by eye. The averages were calculated from those values. The error bars represent the standard deviation between the % engulfed values for each control. The statistical significance was tested using t-Test: Two-Sample Assuming Equal Variance data analysis tool in excel, the calculated P- value was 0.86 which implied that the % of total cells that were engulfed by macrophages in the untreated and treated controls was not statistically different ..... 66

**Figure 3.17.** Graph to show *Candida albicans* SN250 biofilm maturation after 24 hours incubation at  $37^{\circ}\text{C}$ . Controls were an untreated growth control and an addition of

Occidiofungin at growth and attachment stages. The error bars representing the standard deviation between the 12 technical replicates for each concentration. Carried out on a 96 well plate and OD measured using a SpectroStarNano plate reader. The statistical significance was tested using t-Test: Two-Sample Assuming Equal Variance data analysis tool in excel. Statistical significance is represented via the bars with asterixis, these bars represent Controls that are significantly different from each other (P value < 0.05)..... 67

**Figure 3.18.** Graph to show the %Necrosis of different *Candida* species after 90 minutes of treatment at 37°C with Occidiofungin at 3.2, 1.6 and 0.8µgmL<sup>-1</sup>. Each bar is representative of the average from 3 technical repeats. The statistical significance was tested using t-Test: Two-Sample Assuming Equal Variance data analysis tool in excel. Statistical significance is represented via the bars with asterixis, these bars represent Controls that are significantly different from each other (P value < 0.05)..... 68

**Figure 3.19.** Microscopy images to show Alkyne Occidiofungin (Green) and 0.1% Calcofluor White stain (Blue) on *Candida albicans* cells that had been treated with 0.4µgmL<sup>-1</sup> Alkyne Occidiofungin for 50 minutes. Cells were grown overnight in YPD media, the cells where then diluted to a 0.1 OD and grow to log phase. Cells where then treated with Alkyne Occidiofungin for 50 minutes. Images were gathered using an Olympus IX81 fluorecence microscope, with GFP 395/509 nm excitation/emission, at 100x magnification, using an Andor Xyla 4.2 CMOS digital camera..... 69

**Figure 5.1** Diagrams to demonstrate Las17 binding Actin. A - represents Yeast two-hybrid plasmids, where 27 Actin alleles were tested for binding to Las17, all but *act1-104* and *act1-111* interacted with Las17. B - Actin structure highlighting the 27 alleles, Las17 non-interacting alleles are in red. C - Filament model of Actin with *act1-104 residues* in red and *act1-111 residues* in blue (51)..... 73

# 1. Introduction

## *1.1 Current burden of fungal disease*

The global burden of fungal disease has rapidly escalated over recent years, this poses a significant threat to public health. Data suggests that fungal infections are responsible for an approximate 1.5 million deaths annually, with the true burden likely even higher due to gaps in diagnostics and clinical understanding (1). The increasing prevalence of these infections is driven by a multitude of factors, one of the main factors being the emergence of antifungal resistance (2). This undermines the efficacy of existing treatments and highlights the ever more urgent need for new therapeutic options. There are currently no vaccines that are licensed or in clinical study for any fungal disease, therefore in order to minimize death there is a need for improvements in diagnostic practise, antifungal prescribing and a desire for new antifungals to be produced (3).

Fungi are a highly diverse group of organisms that are capable of causing disease in multiple organisms. In humans there are important fungal infections such as Candidiasis, which affect the skin, nails and mucous membranes. In plants, fungal diseases can be widespread due to genetically identical crops, which leads to significant crop damage. Such an example would be Fusarium Wilt, which is caused through various *Fusarium* species, it affects a wide range of plants such as cotton, bananas and tomatoes, and it results in the wilting and death of the infected plants (4). Even in animals fungal infections are still extremely prevalent with infections such as ringworm that is caused by dermatophyte fungi and can be commonly seen with cats, dogs and livestock (5).

With this increase in fungal resistance affecting so many areas in everyday life it has raised a serious concern over the ability of the currently available antifungals to be able to effectively combat these infections. This situation underlines the urgent need for new advancements in

antifungal research and even in antifungal modification, to help towards developing more potent and better targeting antifungal therapies in order to help ease the ever growing pressure surrounding fungal disease.

## ***1.2 Candida infection***

*Candida albicans* is a leading cause of invasive Candidiasis. Candidiasis is a severe infection that affects various systems and organs within the body. It shows particular prevalence within immune compromised individuals, examples of immune compromised individuals would be those undergoing chemotherapy, transplants and even those with HIV/AIDS (6). Invasive Candidiasis can have a mortality rate as high as 50% and this therefore makes it a critical public health concern (7). *Candida* infections also cause a significant economic burden on healthcare systems across the world, this is due to hospital stays being prolonged, along with the requirement of intensive care and antifungal treatments, increasing overall costs (8).

*Candida albicans* has the ability to transition from a commensal organism to pathogenic, this leads to a range of infections from superficial mucosal infections, all the way to life-threatening systemic infections (hyphal form in figure 1.1), this transition can often be attributed to disruptions in the host's immune system and microbiota, hence why immune compromised patients are at higher risk of infection (9,10).

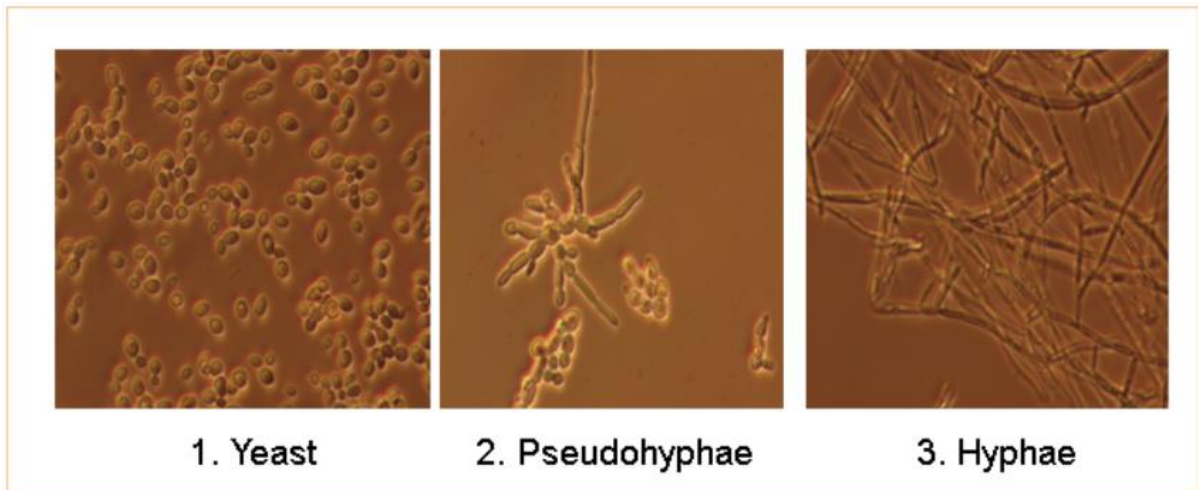


**Figure 1.1.** Image to display the three morphological forms of *Candida albicans*. 1 - Yeast, small round cells that divide by conventional cell division. 2- Pseudohyphae less elongated hyphae, more constricted at septa compared to true hyphae. 3 - True hyphae, elongated cells that do not separate following cell division, separated by specialised septa that allow passage of cytoplasm and other components between compartments (11).

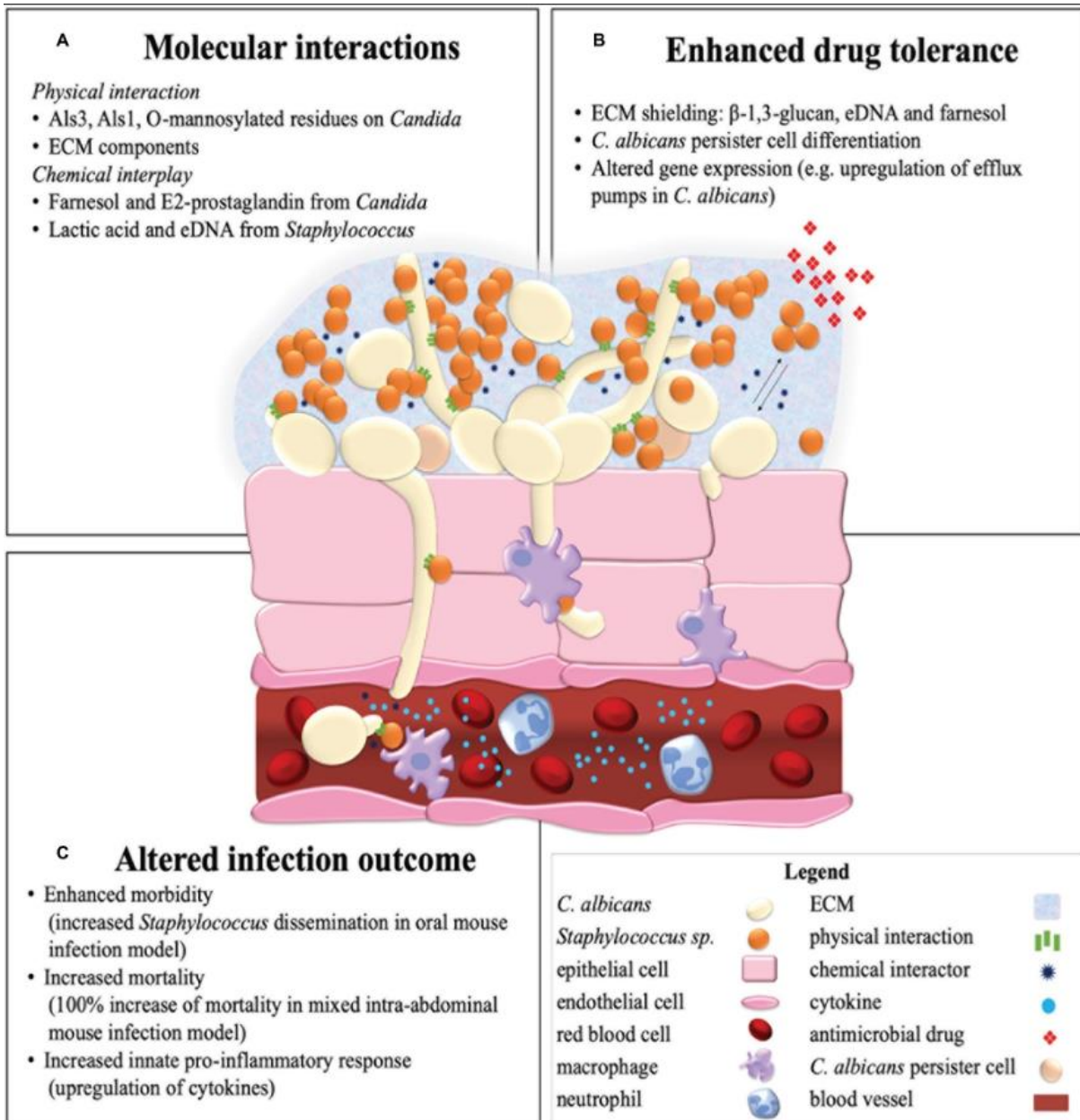


**Figure 1.2.** Illustration to show mixed *C.albicans* and *Staphylococcus* species biofilm within a host environment. Molecular interactions between the two species are represented in: A - invasive endothelial infection with increased antimicrobial drug tolerance. B - altered infection outcome. C - as a result (12).

The ability of Invasive Candidiasis to present itself in varying forms also poses clinical struggle when treating it. The forms include endocarditis (heart infection), Candidemia (bloodstream infection) and more deep-seated infections that can reside in the spleen, liver and kidneys (7). These infections pose serious difficulties in attempting treatment and as a result of this we see them contribute to these high mortality rates.

The WHO published their first ever Fungal Priority Pathogens List of 19 fungal pathogens that pose the greatest threat to health, this list included *Candida albicans*, *Candida auris*, *Candida glabrata*, *Candida tropicalis* and *Candida parapsilosis* with infections such as oral and vaginal thrush becoming increasingly resistant to antifungal treatment (13). This therefore causes concern over more invasive infections, it highlighted the need for better research, diagnostics and effective treatments to combat this resistance and it also indicated that fungal infections are expanding worldwide (13). Due to factors such as increased international travel and global warming, these fungal pathogens are a cause of growing concern (13).

*Candida auris* is also an emerging pathogen that results in nosocomial infections, it also may have invasive infections that are associated with high mortality (14). *Candida auris* is efficiently transmitted person to person and this is not typical within *Candida* species, it is also not considered a resident commensal organism and it is not typically present within the human gastrointestinal tract (15). The colonization of *Candida auris* may persist for many months and possibly indefinitely (15). There is therefore a keen interest to develop antifungals in order to eradicate this pathogen in humans.

Whilst there are antifungal agents such as Polyenes, Azoles and Echinocandins that *Candida albicans* will generally be susceptible to, there is an ever increasing trend in resistance and this is particularly seen in azoles (16). *Candida albicans* has developed a variety of mechanisms that allow it to evade antifungals and make it challenging to develop a vaccine, an example would be its ability to form biofilms (Figure 1.2). Biofilms can cause reduced efficacy of some antifungal treatments and this then complicates how these infections are managed.

There is therefore a clear need for better prevention along with a rapid diagnosis to help better combat these infections. It is therefore vastly important that we employ standard infection control measures, such as washing hands and cleaning the surrounding environment. This is especially important in areas around high-risk patients, to help minimize risk of exposure and

subsequent infection. However this is not always sufficient and is an issue in resource limited healthcare settings. Diagnostics are equally as important on combating *Candida* infection. Rapid and accurate diagnosis can be essential in the timely treatment of *Candida* infections, current diagnostic methods such as blood cultures and molecular assays have limitations in sensitivity and specificity, and this can lead to delays in both diagnosis and treatment (8). Therefore there is a great need for the development of more rapid and reliable diagnostics. This all means that there is an evident importance for comprehensive research. With an emphasis on the need for more robust data on the epidemiology, mortality and complications that are associated with these *Candida* infections (7). This data would be an essential part in understanding the full impact of the disease and this would allow for the development of effective prevention and treatment strategies. Future research should prioritise a focus on understanding the mechanisms of antifungal resistance. There is a keen interest in developing new antifungal agents, this can be accelerated through researching the mechanism of action in current 1st in class antifungals that are undergoing trials.

Current antifungals that are used display different cellular targets to kill fungal cells.

Fluconazole and Itraconazole are examples of two Azoles currently used as antifungals in treatment. These Azoles inhibit the enzyme Lanosterol 14 $\alpha$ -demethylase, which is crucial in the biosynthesis of Ergosterol (17). Ergosterol is an essential component within the fungal cell membrane and by blocking the enzyme this leads to the accumulation of toxic sterol intermediates; these intermediates then disrupt the integrity of the membrane and this is what causes cell death (17). Polyenes, i.e. Amphotericin B, works via binding Ergosterol in the cell membrane of fungal cells and this then forms pores in the membrane, increasing its permeability (18). This causes leakages of intracellular components and subsequently leads to cell death (18). Another antifungal would be Caspofungin which is an Echinocandin.

Caspofungin works via inhibiting enzyme  $\beta$ -1,3-D-glucan synthase, an enzyme that is essential

for the synthesis of  $\beta$ -glucan (19).  $\beta$ -glucan makes up a crucial part of the cell wall, subsequent inhibition leads to the weakening of the cell wall, which causes osmotic instability and ultimately cell lysis (19). Allylamines such as Terbinafine are another type of antifungal. It works by inhibition of the enzyme Squalene epoxidase; this enzyme is involved in Ergosterol biosynthesis and its inhibition leads to the accumulation of Squalene (20). Squalene is toxic to fungal cells, and its accumulation causes disruption in the cell membrane, resulting in cell lysis (20). 5-Fluorocytosine is another example of an antifungal, this compound is converted into 5-Fluorouracil within the fungal cell, this is then incorporated into RNA in the place of Uracil, which causes disruption in protein synthesis (21). As well as this it also inhibits enzyme Thymidylate synthase, resulting in impaired DNA synthesis (21). The combined effect of disruptions in both RNA and DNA synthesis can lead to cell cycle arrest and subsequent apoptosis of the fungal cell (21).

*Candida albicans* also has two different modes of growth that allow it to evade host tissue and immune responses in a host. One of these modes is Hyphal Transition. *Candida albicans* exhibits the ability to transition between yeast and hyphal forms (Figure 1.1), this process is known as Dimorphism and is a key virulence factor (22). The yeast to hyphal transition can be triggered by a number of environmental cues, such as pH, nutrient availability and temperature (22). Hyphal growth involves the elongation of the *Candida albicans* cells into filamentous structures, these structures are what allow it to enter host tissue and evade immune responses, this transition is regulated by a few complex signalling pathways, including the MAPK pathway (Figure 1.3), cAMP-PKA pathway and the Ras1-cAMP-Efg1 pathway (22).

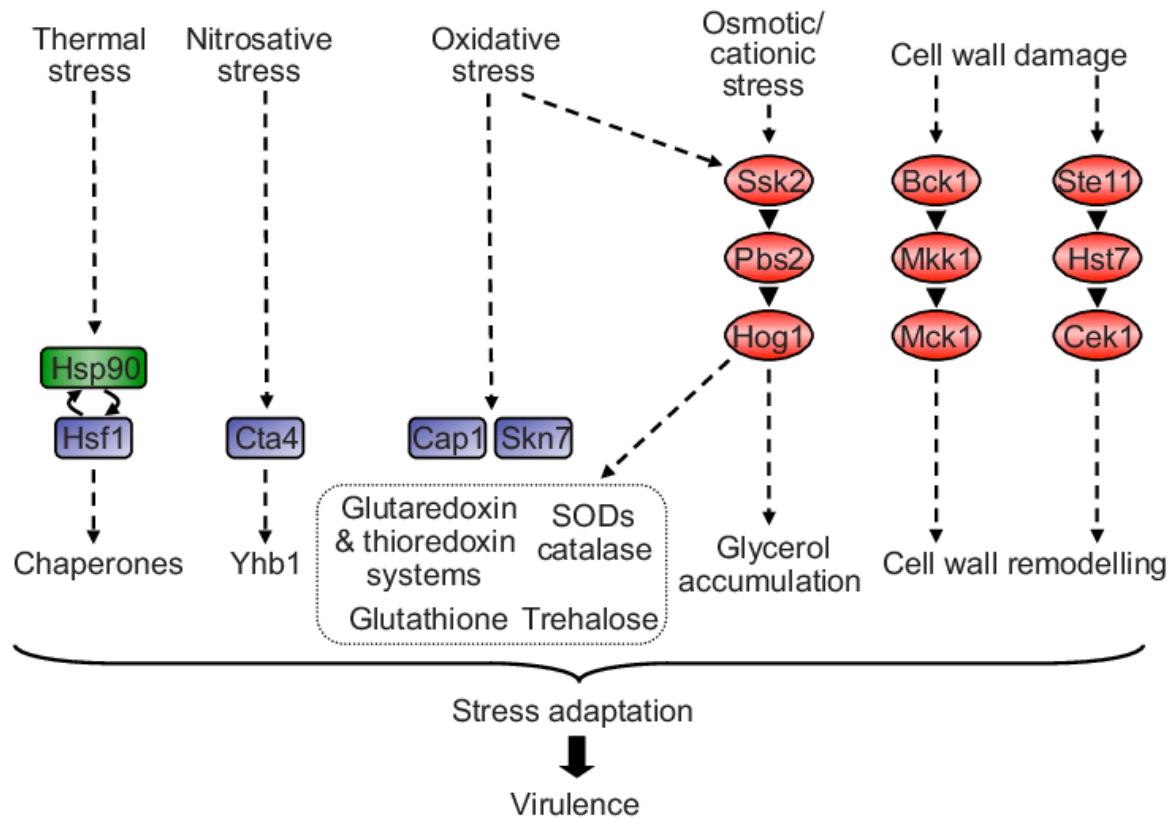


**Figure 1.3.** Image of Conserved stress regulator pathways in *Candida albicans*. MAPK signalling molecules (red), transcription factors (blue), contribute to stress function regulations in *Candida albicans*. Hsf1/Hsp90 form autoregulatory circuit. Heat shock pathway: Hsp90, Hsf1, Nitrosative stress pathway: Cta4, Thb1. Cell integrity Pathway: Bck1, Mkk1, Mkc1. Oxidative stress pathway: Cap1, Skn7, SODs. Hog1 signalling pathway: Ssk2, Pbs2, Hog1 (23).

The other mode of growth seen in *Candida albicans* is biofilm formation. *Candida albicans* possess the ability to form biofilms on both biotic and abiotic surfaces, these can range from mucosal tissue to medical implantations. Formation of the biofilms involve a multi-step process that includes Adherence, Growth and proliferation (Intermediate phase), Differentiation and Matrix formation, and finally Dispersion (See Figure 1.4). Once a biofilm is able to reach matrix formation, it has a highly structured community of cells living within a protective extracellular matrix. This matrix makes it extremely difficult for antifungals to penetrate and destroy the cells inside. The matrix is composed of polysaccharides, proteins and extracellular DNA, with all of these factors contributing to its structural integrity and resistive properties (24).

There is also a genetic control involved in *Candida albicans* biofilm formation. In the initial adherence stage of biofilm formation ALS1 and ALS3 are genes that encode the cell surface glycoproteins that mediate the adherence to the surface and other cells (25). In the intermediate stage where microcolonies are formed, the HWP1 encodes for hyphal development and biofilm stability (26). As well as this EFG1 codes a transcription factor that regulates transition from yeast to hyphal growth (27). In biofilm maturation BCR1 is an essential gene for the maturation itself as well as the expression of other biofilm related genes (28). TEC1 regulates hyphal development and also biofilm formation at this stage (29). At dispersal NRG1 is a gene that represses filamentation and is downregulated during the dispersal of the biofilm (30), also UME6 is a gene that is promoting hyphal growth and is linked to the dispersal of the biofilm at this stage (31).

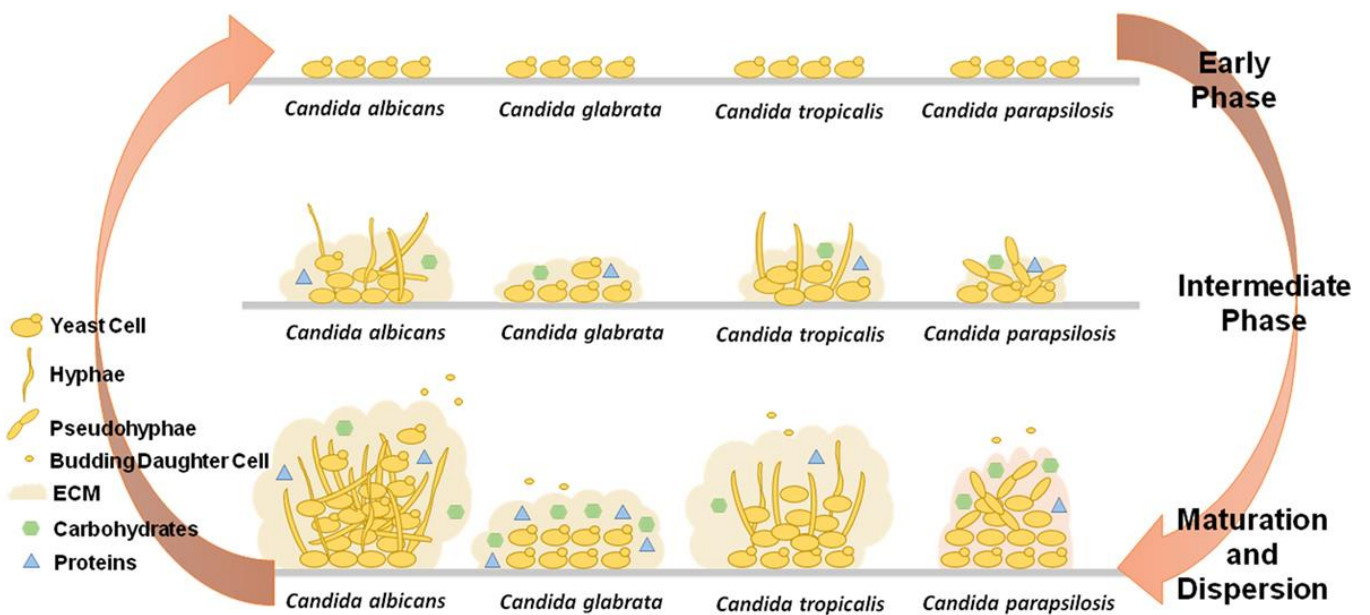
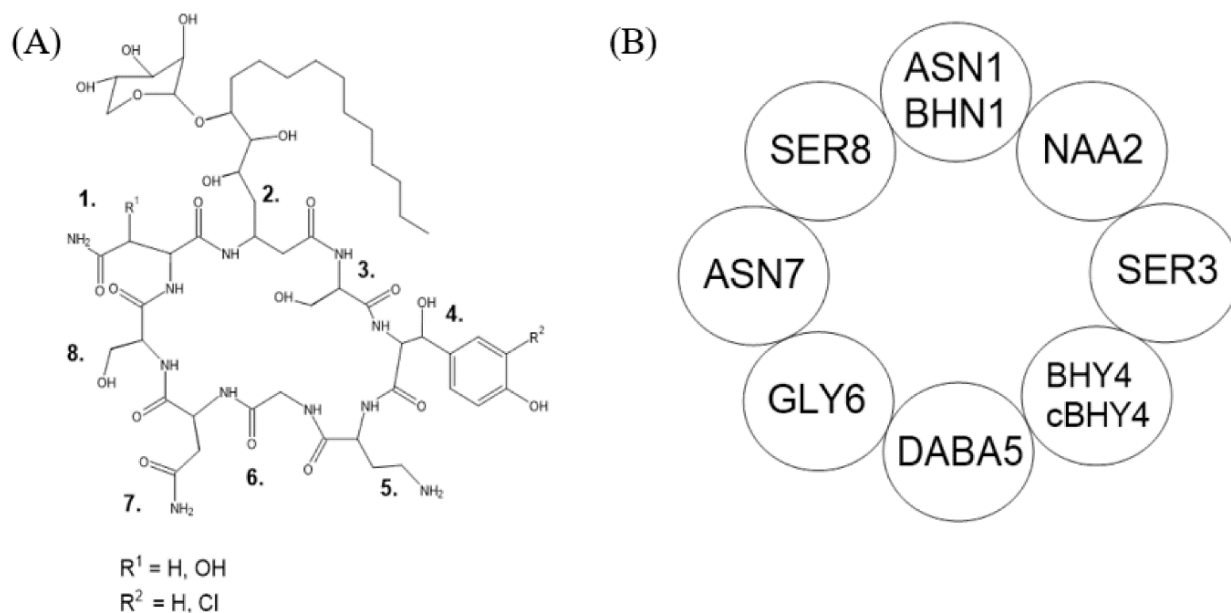


**Figure 1.4.** Diagram to compare stages of biofilm formation, in *Candida albicans*, *Candida glabrata*, *Candida tropicalis* and *Candida parapsilosis*. Highlighting the ability for these strains to produce an extracellular matrix, the various components that reside in the matrix as well as their ability to show different cell morphologies (32).

### *1.3 Occidiofungin – a novel first in class antifungal*

Occidiofungin was discovered by Sano Chemicals in 2009. Bacterial strain *Burkholderia contaminans* MS14 was isolated from soil that suppressed brown patch disease of lawn grass (33). An antifungal compound was then purified from the liquid culture of this bacterium leading to the discovery of a novel fungicide and the compound has been named Occidiofungin (33). High-resolution mass spectrometry data revealed the existence of two structural variants of the antifungal peptide; one having a monoisotopic mass of 1,199.543 Da and the other having a monoisotopic mass of 1,215.518 Da which corresponds to the addition of oxygen to the first compound (33). Given the presence of two structural variants, the variants of the antifungal compound are referred to as Occidiofungin A (1,199.5584 Da) and Occidiofungin B (1,215.5533 Da) (33). In all my experimentations I exclusively used Occidiofungin B (Seen in Figure 1.5).

Occidiofungin has demonstrated a broad spectrum of antifungal activity against various fungal species. Its effectiveness is extensive and it has shown promise in both superficial and systemic fungal infections, therefore making it an interesting prospect for clinical use. As it stands Occidiofungin is currently in clinical development and there are ongoing trials to help evaluate the safety and efficacy of the drug. Occidiofungin has also been fast tracked by the US Food and Drug Administration for treatment in recurrent vulvovaginal Candidiasis (34). However despite its promising potential, there is still a long way to go in Occidiofungin's development. This includes optimisation of its formulation for different types of infections and ensuring its safe for clinical use (34). Therefore there is a great desire to ensure that this drug is further researched so it can be better enhanced and understood. With no definite knowledge of the mode of action of Occidiofungin, this subsequently led to the initiation of this research project to help further progress the understanding of this first in class antifungal.



Occidiofungin A: $R^1 = \text{H, } R^2 = \text{H,}$	$\text{C}_{52}\text{N}_{11}\text{O}_{21}\text{H}_{85}$	1199.59Da
Occidiofungin B: $R^1 = \text{OH, } R^2 = \text{H,}$	$\text{C}_{52}\text{N}_{11}\text{O}_{22}\text{H}_{85}$	1215.59Da
Occidiofungin C: $R^1 = \text{H, } R^2 = \text{Cl,}$	$\text{C}_{52}\text{N}_{11}\text{O}_{21}\text{H}_{84}\text{Cl}$	1233.56Da
Occidiofungin D: $R^1 = \text{OH, } R^2 = \text{Cl,}$	$\text{C}_{52}\text{N}_{11}\text{O}_{22}\text{H}_{84}\text{Cl}$	1249.56Da

**Figure 1.5.** Diagram to show the structure of Occidiofungin A (left hand side) and Occidiofungin B (Right hand side) (33)

### *1.4 Actin as a potential target of Occidiofungin*

The Actin cytoskeleton is a crucial component within eukaryotic cells, playing an essential role in various cellular processes. In yeast cells, the Actin cytoskeleton is composed of dynamic polymers which are involved in processes such as maintaining cell integrity, polarity, division, endocytosis, vesicular trafficking and migration (35). The assembly and disassembly of Actin structures are tightly regulated, this is done by approximately 100 highly conserved accessory proteins that nucleate, elongate, cross-link, and sever Actin filaments (35).

Actin is one of the most abundant and highly conserved proteins in eukaryotes, and it is essential for the survival of most eukaryotic cells. It exists in 2 different states, Filamentous polymeric (F-Actin) and Globular monomeric (G-Actin) (35). Yeast cells have the ability to assemble 3 distinct Actin structures: Cortical Actin patches, Actin cables, and the Actomyosin

ring. Cortical Actin patches (which are a point of focus in my experimentation) are dense dendritic networks of branched Actin filaments nucleated by the Arp2/3 complex and are involved in Clathrin-mediated endocytosis (Figure 1.6)(35). Actin cables are polarised linear bundles of parallel actin filaments which extend along the axis of the yeast cell, they serve as tracks for polarised transport of various cell cargo (35).

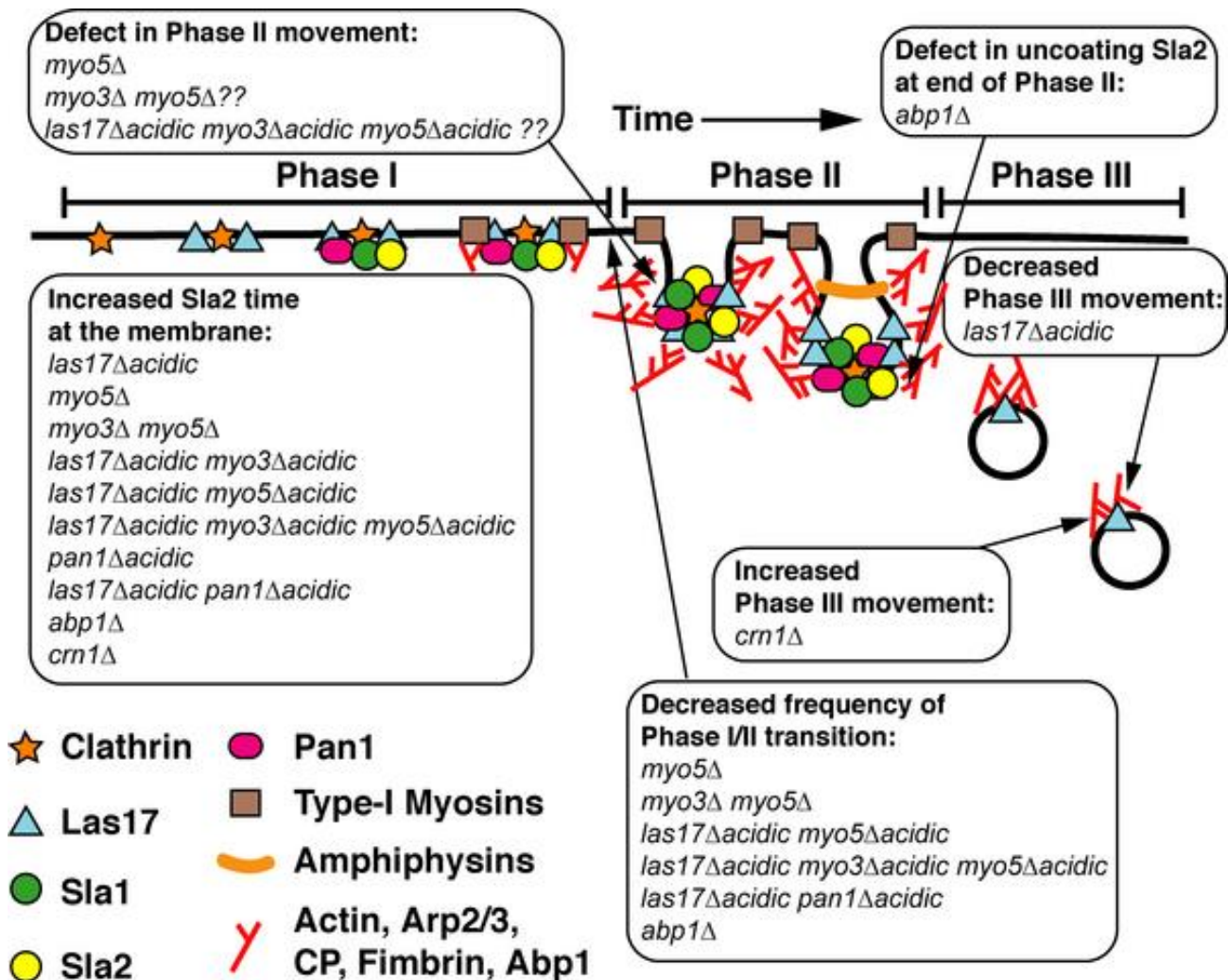


**Figure 1.6** Diagram to show a model of Endocytosis and Actin patch assembly. Phase I - indicates where most Arp2/3 regulators will promote the assembly to establish an Actin network with suitable filament lengths and branch density. Phase II - The Arp2/3 regulation complex, there are no single regulator mutation affects this stage, but mutations in WASp/Las17, Myo3 and in Myo5 disrupt movement. Phase III - Actin filaments that were nucleated at the Actin patch, drive vesicle movement in the cytoplasm (36).

Actin Cortical patches are a focus of part of my research, therefore there is a keen interest in their role in endocytosis. One of their roles is Initiation, in which the process of endocytosis

begins with the recruitment of the endocytic adaptor proteins (Clathrin and other Clathrin-associated proteins) to the plasma membrane, this then assists in the recognition of the cluster cargo molecules that need to be internalised (37). The patches are also involved in Actin nucleation and polymerisation, in which the Arp2/3 complex is activated by nucleation promoting factors such as Las17 (the yeast homologue of mammalian WASp) which then leads to the nucleation of new Actin filaments, these filaments are then able to grow and branch off, forming a dense network that then pushes against the plasma membrane, which subsequently drives the invagination of the membrane to form an endocytic vesicle (38,39,40). Actin Cortical patches are also involved in vesicle scission and movement. Vesicle Scission involves the Actin network providing the force necessary for the scission of the endocytic vesicle from the plasma membrane, this is facilitated by the coordination action of Actin binding proteins and motor proteins (for example myosin), this then generates the mechanical force required for vesicle release (41). Vesicle Movement then takes place after scission, the Actin cortical patches continue to play a role even at this point via the movement of the endocytic vesicle into the cytoplasm, in which the vesicle is transported along Actin cables to its destination within the cell (36).

It is important to note that Actin Stabilisation has also been linked with cell death. There are a multitude of reasons as to why this occurs. One reason is that it leads to the disruption of cellular processes, whereby it interferes with processes such as endocytosis, vesicular trafficking and cytokinesis, without proper regulation of these processes this can lead to cellular dysfunction which then results in cell death (42). Actin stabilisation can also induce apoptosis within yeast cells, this was evidenced by the presence of apoptotic markers such as DNA fragmentation and chromatin condensation in cells that has stabilised Actin (42). It is also noted that under oxidative stress conditions that Actin will form further aggregates in order to stabilise filaments, these aggregates can be detrimental to the viability of the cell as they disrupt normal

function of the cytoskeleton, this accumulation is also associated with an increase in cellular levels of reactive oxygen species (ROS) which will lead to damage of cell components and subsequent apoptosis (42). Actin also interacts with signalling pathways, the stabilisation of Actin can affect many of these pathways, including MAPK, TORC1, TORC2 and Ras/cAMP/PKA pathways (42). These pathways are crucial for the survival and proliferation of the cell and the disruption of these Actin dynamics can lead to hyperactivation or inhibition of the pathways mentioned, this can lead to a variety of negative cellular effects such as mitochondrial dysfunction and ROS accumulation and ultimately this is what then leads to cell death (42). The Actin cytoskeleton plays a key role in clearance of damaged organelles and proteins, utilising processes such as autophagy. Stabilized Actin filaments will impair these clearance mechanisms and this results in the accumulation of damaged cellular components which then triggers apoptotic cell death (42).

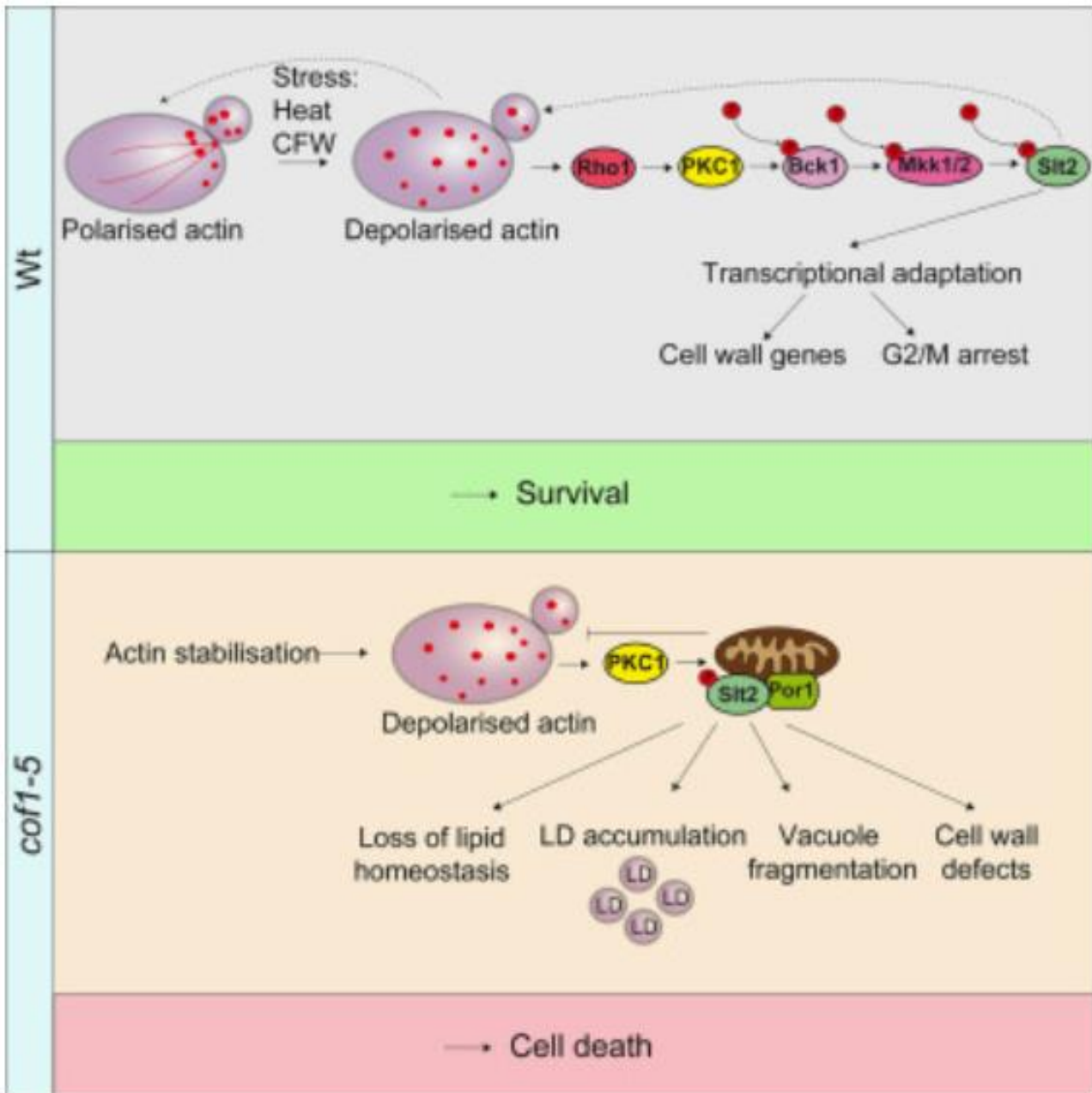


**Figure 1.7** Diagram of VDAC-dependant MAPK signalling. In Wild type cells the Actin cytoskeleton is polarised along the mother-bud axis, a cell wall stress then depolarises the cytoskeleton, this triggers the Cell wall integrity MAPK pathway, leading to transcriptional adaptation of cell wall genes, promoting cell survival. In *cof1-5* cells Actin is stabilised and chronically depolarised, constantly triggering the Cell wall integrity pathway, Pkc1 and Slt2 localize to the mitochondrion (Por1 dependant), this causes loss of lipid homeostasis, lipid droplet accumulation, vacuole fragmentation and cell wall defects (43).

A research paper from 2022 suggested that Occidiofungin targets Actin and described this as its mode of action to explain its potent effect (34). To investigate this the research conducted a

series of experiments to elucidate this hypothesis. The research involved *in vitro* studies in which yeast cells were treated with Occidiofungin, they then looked to observe whether this treatment displayed an effect on Actin filaments by monitoring cellular processes. Some of their key experiments included binding studies, in which they aimed to determine whether Occidiofungin binds directly to Actin, the results from this experiment indicated that there was a strong interaction between the two (34). They also conducted microscopy analysis in which they visualised the organisation of Actin filaments within the treated cells. They observed significant disruption in the structure of Actin filaments, supporting their hypothesis of Occidiofungin targeting Actin (34). The paper also highlighted the use of apoptosis assays, where they conducted assays that detected markers of cell death such as DNA fragmentation and chromatin condensation in cells that were treated with Occidiofungin (34). The presence of these markers in their experimentation suggested that the disruption of Actin was leading to apoptotic cell death and further supported their hypothesis (34). The research paper stated that that unlike other Actin-binding compounds Occidiofungin does not inhibit the Actin polymerisation or depolymerisation. They instead suggested that it disrupts higher order Actin functions, this therefore provided a novel mechanism of action that if true would circumvent the existing resistance mechanisms of yeast cells (34). Overall this research paper posed a strong hypothesis on the mode of action of Occidiofungin, making Occidiofungin a strong candidate for the development of new antifungal therapies. Occidiofungin does however require further research in order to support this hypothesis.

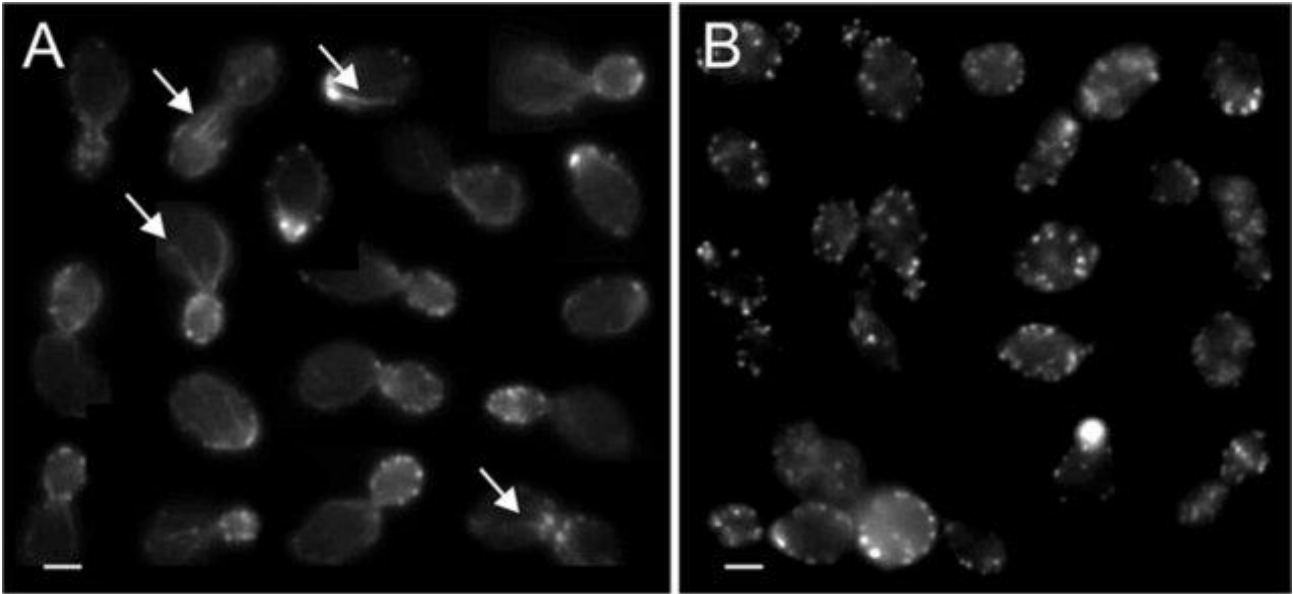


**Figure 1.8.** Image to show Effects of Occidiofungin exposure on the integrity of Actin cables in *S. cerevisiae* cells. A represents the DMSO control, Actin patches and cables are visible from arrows. B represents Occidiofungin treatment at 0.5x the MIC for 30 minutes, cables are lost and Actin aggregates accumulate, scale bars represent 2 $\mu$ m (44).

### 1.5 Cofilin

Cofilin is an Actin-binding protein that controls Actin dynamics and has also been linked with mitochondrial signalling pathways that control drug resistance and cell death (43). Cofilin-driven chronic depolarization of the Actin cytoskeleton activates cell wall integrity mitogen-activated protein kinase (MAPK) signalling and disrupts lipid homeostasis in a voltage-dependent anion channel (VDAC) dependent manner (43). Expression of the *cof1-5* mutation, which reduces the dynamic nature of Actin, triggers loss of cell wall integrity, vacuole fragmentation, disruption of lipid homeostasis, lipid droplet (LD) accumulation, and the promotion of cell death (43). The integrity of the Actin cytoskeleton is therefore essential to maintain the fidelity of MAPK signalling, lipid homeostasis, and cell health in *S. cerevisiae* (43). The phenotype displayed here is the same phenotype of depolarised Actin patches that were a part of the research paper suggesting Actin was a target (34). Therefore this pathway is of key interest and is linked to experimentations that I undertook in my research.

## ***1.6 Aims of my research***

This research aims to explore the novel antifungal properties of Occidiofungin, with a particular focus on its mechanism of action involving the Actin cytoskeleton to determine whether the current ideologies are an accurate representation of Occidiofungin's mode of action.

The objectives for my study involved: Characterization of the mechanism of action of Occidiofungin, in order to elucidate how and if Occidiofungin interacts with Actin and disrupts higher-order Actin mediated cellular functions, which subsequently then leads to apoptosis. I investigate the broader antifungal spectrum, assessing *in vitro* and *in vivo* effectiveness of Occidiofungin against different *Candida* species that are prevalent in serious fungal infections in our current healthcare system. Fungal specificity is also investigated; to determine the specificity of Occidiofungin for fungal cells over mammalian cells, this was done through the use of haemolysis assays as well as using *Galleria mellonella* infection models to test Occidiofungin for other cellular toxicity. These assays helped to evaluate the safety and selectivity of Occidiofungin as an antifungal agent.

## 2. Materials and Methods

### *2.1 Yeast strains and Growth*

#### Medias/Stains/Reagents

**YPD Media** - 8g Peptone, 4g Yeast Extract, 380mL MiliQ Water, 20mL Glucose.

**YPD Agar Media** - 8g Peptone, 4g Yeast Extract, 8g 2% Agar, 380mL MiliQ Water, 20mL Glucose.

**Blood Agar** - 8g Peptone, 4g Yeast Extract, 8g 2% Agar, 380mL MiliQ Water, 10mL Sheep Blood.

**Uracil Dropout Agar** - 190mL distilled water, 1.35g Yeast Nitrogen Base (Kaiser, Foremedium), 0.3g yeast synthetic dropout Kaiser media (-uracil), 10mL 40% glucose, 4g 2% Agar.

**DMEM Cell Culture Media** - Gibco™ DMEM, high glucose, GlutaMAX™ Supplement, pyruvate. From fischer Scientific.

**PBS** - 800ml distilled water, 8g NaCl, 1.44g Na<sub>2</sub>HPO<sub>4</sub>, 0.2g of KCl, 0.24g KH<sub>2</sub>PO<sub>4</sub>, Bring the pH to 7.4 or 7.2 using HCl, distilled water added until the total volume reaches 1 litre.

**Calcofluor White** - Used at a concentration of 1g/L.

**XTT** - Sourced from Sigma Aldrich and used as per the manufacturers guidelines (56).

**Table 2.1.** Table containing all the Yeast strains used in experimentation over the course of the project. *ACT1* Mutants (45). *Candida albicans* - *SN250* (46).

Strain	Genotype
<i>Saccharomyces cerevisiae</i> - <i>BY4741</i>	<i>MATa his3Δ1 leu2Δ0 met15Δ0 ura3Δ0</i>
<i>Saccharomyces cerevisiae</i> - <i>Wt</i>	<i>MATa his3D200 leu2-3, 112 lys2::HIS3 ura3-52 ade2</i>
<i>Saccharomyces cerevisiae</i> - <i>act1-105</i>	<i>MATa act1-101::HIS3 bar1D::LYS2 his3D200 ura3-52 lys2-801 leu2-3, 112 ade2</i>
<i>Saccharomyces cerevisiae</i> - <i>act1-119</i>	<i>MATa act1-119::HIS3 bar1D::LYS2 his3D200 ura3-52 lys2-801 leu2-3, 112 ade2</i>
<i>Saccharomyces cerevisiae</i> - <i>act1-120</i>	<i>MATa act1-120::HIS3 bar1D::LYS2 his3D200 ura3-52 lys2-801 leu2-3, 112 ade2</i>
<i>Saccharomyces cerevisiae</i> - <i>act1-124</i>	<i>MATa act1-124::HIS3 bar1D::LYS2 his3D200 ura3-52 lys2-801 leu2-3, 112 ade2</i>
<i>Saccharomyces cerevisiae</i> - <i>act1-122</i>	<i>MATa act1-122::HIS3 bar1D::LYS2 his3D200 ura3-52 lys2-801 leu2-3, 112 ade2</i>
<i>Saccharomyces cerevisiae</i> - <i>act1-125</i>	<i>MATa act1-125::HIS3 bar1D::LYS2 his3D200 ura3-52 lys2-801 leu2-3, 112 ade2</i>
<i>Saccharomyces cerevisiae</i> - <i>act1-129</i>	<i>MATa act1-129::HIS3 bar1D::LYS2 his3D200 ura3-52 lys2-801 leu2-3, 112 ade2</i>
<i>Saccharomyces cerevisiae</i> - <i>act1-20</i>	<i>MATa act1-20::HIS3 bar1D::LYS2 his3D200 ura3-52 lys2-801 leu2-3, 112 ade2</i>
<i>Saccharomyces cerevisiae</i> - <i>act1-3</i>	<i>MATa act1-3::HIS3 bar1D::LYS2 his3D200 ura3-52 lys2-801 leu2-3, 112 ade2</i>

<i>Saccharomyces cerevisiae</i> - <i>act1-117</i>	<i>MATa act1-117::HIS3 bar1D::LYS2 his3D200 ura3-52 lys2-801 leu2-3, 112 ade2</i>
<i>Saccharomyces cerevisiae</i> - <i>act1-135</i>	<i>MATa act1-135::HIS3 bar1D::LYS2 his3D200 ura3-52 lys2-801 leu2-3, 112 ade2</i>
<i>Saccharomyces cerevisiae</i> - <i>act1-104</i>	<i>MATa act1-104::HIS3 bar1D::LYS2 his3D200 ura3-52 lys2-801 leu2-3, 112 ade2</i>
<i>Saccharomyces cerevisiae</i> - <i>act1-111</i>	<i>MATa act1-111::HIS3 bar1D::LYS2 his3D200 ura3-52 lys2-801 leu2-3, 112 ade2</i>
<i>Saccharomyces cerevisiae</i> - <i>act1-4</i>	<i>MATa act1-4::HIS3 bar1D::LYS2 his3D200 ura3-52 lys2-801 leu2-3, 112 ade2</i>
<i>Candida albicans</i> - <i>SC5314</i>	<i>N/A Clinical Isolate</i>
<i>Candida albicans</i> - <i>SN250</i>	<i>arg4Δ/arg4Δ, leu2Δ/LEU2, his1Δ/HIS1, URA3/ura3Δ, IRO1/iro1Δ</i>
<i>Candida albicans</i>	<i>N/A Clinical Isolate</i>
<i>Candida parapsilosis</i>	<i>N/A Clinical Isolate</i>
<i>Candida dubliniensis</i>	<i>N/A Clinical Isolate</i>
<i>Candida glabrata</i>	<i>N/A Clinical Isolate</i>
<i>Candida tropicalis</i>	<i>N/A Clinical Isolate</i>

## ***2.2 Minimum Inhibitory Concentration (MIC) Assay***

Cells were inoculated in 5mL of YPD media and grown overnight in a shaking incubator at 30 or 37°C as required. 1mL of each overnight culture was pelleted at 4000 rpm for 4 mins and washed twice with 1 ml PBS. Cells were then resuspended in 1ml of PBS and 50µL was added to 950µL of PBS and the absorbance measured at 600nm in a spectrophotometer. An appropriate volume of OD600 0.2 cell solution was prepared in YPD media (typically a 10mL volume was made to accommodate for a 96 well plate experiment). 100µL of YPD was then added to each of the wells of a 96 well plate. 1mL of a 4x drug concentration was made by diluting the stock concentration of Occidiofungin in the required volume of PBS (Concentrations varied dependant on experiment, MIC assays typically used a 12.8µgmL<sup>-1</sup> 3x starting Occidiofungin concentration). 100µL of this was then added to each of the wells in column A. This was then serially diluted 2 fold down the rows, meaning each column was half the previous columns solution, this was done using a multichannel pipette at 100µL. 100µL of OD 0.2 cell solution in YPD was then added to columns 2-9, rows B-G, leaving a media blank and cell blank in columns 10 and 11, as well as no Occidiofungin being added in these columns (the outer wells were ignored due to evaporation). The plate was then placed into a SpectroStarNano for 24 hours at 30/37°C. Data was exported into Excel for analysis.

## ***2.3 Assessment of ROS accumulation and Necrosis using Flow Cytometry***

Cells were inoculated in 5mL YPD media in test tube, then placed in a shaking incubator at 30°C overnight. Once the cells had grown overnight, the culture was diluted to an OD of 0.2. The OD 0.2 solution was then grown to log phase for 3 hours in a shaking incubator at 30°C, Occidiofungin was then added at 0.24µgmL<sup>-1</sup> for 60 minutes, I then added 1 µL of 10 mM H2DCFDA , before adding 3µL of 1mgmL<sup>-1</sup> Propidium Iodide and analysed this sample using

a BD Accuri™ C6 Plus Flow Cytometer using FITC and PER-CP detectors, which counted a 15,000 cell population. Excel was then used for analysis.

For alternate experimentation, the test tube (prior to addition of stains) was split into three 5mL aliquots using sterile falcon tubes. One aliquot was used to test the MIC of Occidiofungin (0.24ug/mL) as well as be stained with H2DCFDA (stains free radical oxygen species). Another contained only the stain. The final aliquot was a control that contained neither Occidiofungin nor H2DCFDA. These aliquots were then treated for an hour in a shaking 30/37°C incubator. Once the hour was completed the falcon tubes were spun down at 4000RPM for 4 minutes. The pellet was resuspended in 1mL of PBS, this was then split into two 500uL aliquots. One of these aliquots was then stained with Propidium Iodide (stains DNA and RNA, highlighting necrotic cells in suspension). The aliquots were then run through the flow cytometer, ensuring they were vortexed before every run. Data was then be collected and analysed.

Dependant on the experiment, H2DCFDA would not always be used. The main stain used was PI stain in order to gather results for the necrosis assays. H2DCFDA was only used for testing the ROS level.

#### *2.4 Analysis of lipid droplet number by fluorescence microscopy*

Cells were grown in YPD media at 30°C to log phase, a 1mL (0hr) sample was taken and placed into an eppendorf, washed twice using PBS and cells were then exposed to Occidiofungin at 0.24µgmL<sup>-1</sup> for 2 hours. Cells were incubated with Bodipy in a dark area for 10 minutes before being viewed on an Olympus IX81 fluorescence microscope using excitation at 505nm emission 515 filters. Occidiofungin treatment controls were collected and stained every hour for comparison. 2.5µL of the sample was then placed onto a microscope slide. 2.5µL of Calcofluor White solution was then added to stain the sample on the slide. A cover

slip was then placed onto the slide sample. Cells were viewed on an Olympus IX81 fluorescence microscope using GFP 395/509 nm excitation/emission illumination and 100x magnification, images captured using an Andor Xyla 4,2 CMOS camera using Metamorph image acquisition software.

### ***2.5 Alkyne Occidiofungin imaging***

*Candida albicans* cells were grown overnight at 37°C in a shaking incubator. Cells were then diluted to a 0.1 OD and then grown to log phase in the same incubator for 2 hours. The cells were then treated with 0.4 µg mL<sup>-1</sup> Occidiofungin for 50 minutes at 37°C in a shaking incubator. This sample was then spun down at 4000 RPM for 3 minutes, supernatant was then removed using a 1 mL pipette and 500 µL of PBS was then added. 2.5 µL of this solution was then added to a microscope slide along with 2.5 µL of Calcofluor White solution. Images were gathered using an Olympus IX81 fluorescence microscope, with GFP 395/509 nm excitation/emission, at 100x magnification, using an Andor Xyla 4.2 CMOS digital camera.

### ***2.6 Yeast plasmid transformation***

Plasmid was prepared using a Qiagen miniprep kit as per the manufacturer's instructions, the plasmid was stored in DH5α (Δ(argF-lac)169, φ80dlacZ58(M15), ΔphoA8, glnX44(AS), deoR481, rfbC1, gyrA96(NalR), recA1, endA1, thiE1 and hsdR17) *E.coli*. The plasmid containing GFP-ABP1 (pCG) contained an *ACT1* promoter and terminator, a *URA3* gene for selection in auxotrophic yeast, an ampicillin resistance gene for selection in *E.coli*, a CEN (low copy) origin of replication and this was kindly gifted to the lab from the lab of Professor

David Drubin (University of California, Berkley). The plasmid was purified according to Qiagen Miniprep kit instructions.

Drop out Uracil agar plates were made in preparation for plasmid selection. To do this I added 190mL of water, yeast nitrogen base (Foremedium, 1.35g), amino acid supplement lacking Uracil (Foremedium, 0.3g) and Agar (4g) to a glass bottle with a screw lid, this solution was then autoclaved. Once it was autoclaved and slightly cooled I added 10mL of 40% Glucose. The mixture was then poured into petri dishes at equal volumes and allowed to set.

*Saccharomyces cerevisiae* BY4741 cells were grown in 5mL of YPD media overnight at 30°C in a shaking incubator. After this 1mL of cell solution was placed into an eppendorf, this was then spun down and washed twice with PBS. The remaining pellet was then resuspended in PBS and 50µL of this was added to a cuvette along with 950µL of PBS and this was read in a spectrophotometer to acquire the OD600 of the cell solution. Once known, a 5mL OD 0.1 solution was then made up in a falcon tube and grown in the 30°C shaking incubator until it had an OD of 0.6-1 (around 2-3 hours). Once the cells were in log phase they were harvested. This was done via centrifuging the Falcon tube for 5 minutes at 3000RPM. The supernatant was then discarded and the cell pellet was resuspended in 25 mL of sterile water. The cells were then washed, this was done through centrifuging the falcon tube again for 5 minutes at 3000RPM, supernatant was discarded and the pellet was then resuspended in 1mL of 0.1M lithium acetate (LiAc) solution. This cell suspension was then incubated for 30 minutes at 30 °C in a shaking incubator.

A transformation mixture was then made up in a sterile microcentrifuge tube, via the addition of, 100µL of competent cells mixed with 10µL of Plasmid DNA (1µg), 50 µL of 50% polyethylene glycol, 10µL of 1M LiAc, and finally 10µL of 1mgmL<sup>-1</sup> single-stranded carrier DNA. The mixture was heat shocked at 42°C for 30 minutes. After heat shock the cells were then centrifuged at 3000 rpm for 1 minute. Pellet resuspended in 1mL of YPD media and

incubated for an hour at 30°C. The transformed cells were then spread onto the drop out uracil agar plates and these plates were then incubated at 30°C for 3 days. Single colonies were re-streaked onto fresh drop out URA plates for use.

## ***2.7 Haemolysis Assay***

Blood agar plates were prepared by adding 200mL of 2% agar solution in YPD media, this solution was then autoclaved. Once it had autoclaved it was placed into a 50°C water bath in order to keep it liquified but at a suitable temperature for the addition of the sheep blood. Once it was cooled 10mL of sheep blood was added to the agar. The mixture was then gently swirled in order to ensure it was evenly mixed, it was then poured into petri dishes and allowed to solidify at room temperature. Four different concentrations (35,3.5,0.35 and 0.035 $\mu\text{g mL}^{-1}$ ) of Occidiofungin were prepared and 15 $\mu\text{l}$  added to a sterile filter disc placed on the agar surface. A 10% Sodium dodecyl sulphate (SDS) solution was then prepared as a positive control. Plates were incubated in a 37°C incubator for 24 hours and imaged using a Samsung Galaxy S21 Ultra.

## 2.8 *Galleria mellonella* infection and toxicity assay

Solutions to be injected into *Galleria mellonella* were prepared as follows:

- 35 $\mu\text{g mL}^{-1}$  Occidiofungin - prepared from the stock Occidiofungin solution using PBS to dilute, to make a 500 $\mu\text{L}$  sample.
- Occidiofungin 1.6  $\mu\text{g mL}^{-1}$  - prepared from the stock Occidiofungin solution, diluted with PBS, to make a 1mL sample. A 2x Concentration was made up at 500 $\mu\text{L}$  for the pre-treated control.
- 1.1% DMSO solvent control- this was made from the addition of 1.1 $\mu\text{L}$  100% DMSO to 98.9 $\mu\text{L}$  of sterile water in an eppendorf tube.
- PBS Control - Taken from PBS stock.

After the Occidiofungin and control solutions were prepared, *Galleria mellonella* of equivalent size and health were selected and placed into petri dishes that contained filter paper.

Dependant on the experiment these dishes would contain 10 or 15 larvae each. Using a small syringe 10 $\mu\text{L}$  of appropriate solution was injected into the bottom left proleg. The injections made for each experiment are as follows; for the *Candida* Infected control, Cells were grown overnight in YPD media in a 37°C incubator, they were then diluted to a 0.1OD in 1mL and this is what was injected. *Candida* pre-treated control followed the same initial incubation and similar dilution of the *Candida*, once at a 0.2 OD the 1mL was split into two 500 $\mu\text{L}$  eppendorf's, 500 $\mu\text{L}$  of 3.2 $\mu\text{g mL}^{-1}$  Occidiofungin was then added to one of the eppendorf's, this was then incubated at 37°C for 90 minutes, after incubation the sample was injected. *Candida* and Occidiofungin that were injected into opposite prolegs saw the same *Candida* growth and dilution to an OD of 0.1, this was injected into the bottom left pro leg and the 1.6 $\mu\text{g mL}^{-1}$  Occidiofungin was injected into the bottom right proleg. Once all the injections had taken place the larvae were kept in the dishes and placed into a 37°C incubator. I then assessed the worms

every 24 hours for 7 days and scored them. Data was plotted on a Survivability plot using excel software.

## ***2.9 Macrophage engulfment assay***

### ***Preparation of Macrophages***

RAW 264.7 cell line macrophages (a mice macrophage cell line) were used in this experiment. The macrophages were cultured in DMEM (Dulbecco's Modified Eagle Medium). The cells were maintained at 37°C in a 5% CO<sub>2</sub> incubator. The macrophages were split every day in order to maintain optimal growth conditions. The cells were split in a 1:2 ratio when they reached approximately 80% Confluence and diluted to  $1.5 \times 10^5$  for experimentation.

### ***Preparation of yeast cells***

*Candida albicans* cells expressing *mtGFP* were cultured overnight in YPD medium at 30°C in a shaking incubator. These cells were then diluted to an OD 1.0 in 5mL of YPD medium. These cells were then treated with  $0.8 \mu\text{g mL}^{-1}$  Occidiofungin for a 2 hour period. Once completed the cells were washed 3 times in PBS. The cells were then counted using a haemocytometer and  $7.5 \times 10^5$  cells/mL were used in the engulfment experiment.

### ***Engulfment assay***

The diluted  $1.5 \times 10^5$  cells/mL macrophage suspension was added to the wells of an 18-well plate, with 8 wells receiving 1mL of the suspension. The plate was then placed into a 37°C incubator with 5% CO<sub>2</sub> and incubated for a 24 hour period. The prepared  $7.5 \times 10^5$  cells/mL *C.albicans* suspension was then added at the calculated volume (1mL) to the macrophage cultures to ensure a 5:1 ratio. The co-culture was then incubated for 1 hour in the 37°C 5% CO<sub>2</sub> incubator. After the incubation period the culture medium was removed and the wells

were gently washed with PBS, the samples were then immediately prepped with a thin PBS layer in the wells to allow for visualisation under the microscope. Phagocytosis was then quantified manually using the ImageJ software. The percentage uptake was calculated by determining the number of internalized *C.albicans* cells relative to the total cell number. At least 200 *C.albicans* cells were counted per localised image.

### ***2.10 Candida albicans Biofilm Assay***

*C.albicans* cells were inoculated in 5mL of YPD media and incubated overnight in a 37°C shaking incubator. 100µL of 50% DBS (Donor Bovine Serum, Thermofisher) solution was added to each well in a 96 well plate, the plate was then incubated for 30 minutes in a 30°C incubator. Once completed the plate was washed twice with 1x PBS solution, this was done via quickly upturning the plate and using paper towels to absorb the liquid (100µL of PBS was added to each well for one wash). After the wash was complete the overnight *C.albicans* culture was centrifuged for 5 mins at 3000 RPM, the supernatant was then removed and the resulting pellet was then resuspended in 1x PBS, this was repeated so the culture had been washed twice and diluted to an OD of 0.2. 100µLs was then added to each well for 90 minutes to attach before washing twice with 100µLs of PBS to remove cells that had not adhered. 100µLs of RPMI media was then added and biofilms were left to grow for 24 hours at 37°C in a shaking incubator. To assess the effects on *C.albicans* attachment, Occidiofungin was added during the 90m min attachment phase at a concentration of either 6.4 or 3.2µgmL<sup>-1</sup>. To examine the effects on biofilm maturation Occidiofungin was added at the same concentrations following the 90 minute attachment phase. Plates were then incubated for 24 hours in a 37°C shaking incubator. After the incubation period the plates were washed twice with 1x PBS to remove any non-adhered cells. After this the XTT reagent (Roche) was added at 100µL to each of the wells.

To make the XTT reagent I added 30 $\mu$ L of decoupling reagent to an eppendorf containing 1.5mL of labelling reagent (Roche), I then inverted this to mix. Once mixed I added 500 $\mu$ L of the mixture to a falcon tube containing 9500 $\mu$ L of PBS. The falcon tube was then gently inverted and 100 $\mu$ L of this solution was added to each of the wells in the plate. The plates were then incubated at 37°C for 4 hours, after the incubation period 90 $\mu$ L of the solution was transferred from each well into a new plate, respective of the well position. These new plates were then read at 492nm in a plate reader and the data was then collected and analysed on excel software.

## 3 Results

### *3.1 Occidiofungin MIC<sub>50</sub> determination in Saccharomyces cerevisiae cells.*

To investigate the effect of Occidiofungin we wished to employ the model yeast *S.cerevisiae*. We therefore established an effective concentration range to work within using the Wt reference strain. The MIC<sub>50</sub> for Occidiofungin was determined using a growth curve and averaging the absorbance of 6 technical replicates at each concentration (Figure 3.1). This was done using a 96 well plate and serially diluting the Occidiofungin with 6 replicates at each concentration, using a starting concentration of 3.2 µg mL<sup>-1</sup>. The MIC<sub>50</sub> is defined as the concentration of Occidiofungin that it takes to inhibit the normal growth of *S.cerevisiae* by 50% in a 24 hour period. We observed a visible decrease in growth of *S.cerevisiae* from the untreated cells at concentrations of 0.2 µg mL<sup>-1</sup> to 3.2 µg mL<sup>-1</sup>, with there being no growth at all from concentrations of 1.6 & 3.2 µg mL<sup>-1</sup>. The assay established the MIC<sub>50</sub> of Occidiofungin to be 0.35 µg mL<sup>-1</sup> which correlated with the graph above as we see the area under the graph value becomes reduced by just over half the normal growth value at around a -0.5 Log concentration of Occidiofungin, the point on the graph representing the 0.4 µg mL<sup>-1</sup> Occidiofungin concentration. The MIC was not determined according the EUCAST standards and instead via calculating the Area Under the Curve and comparing this at different drug concentrations. This method provides a more accurate assessment of biomass as opposed to a visual inspection of when growth is not present by eye.

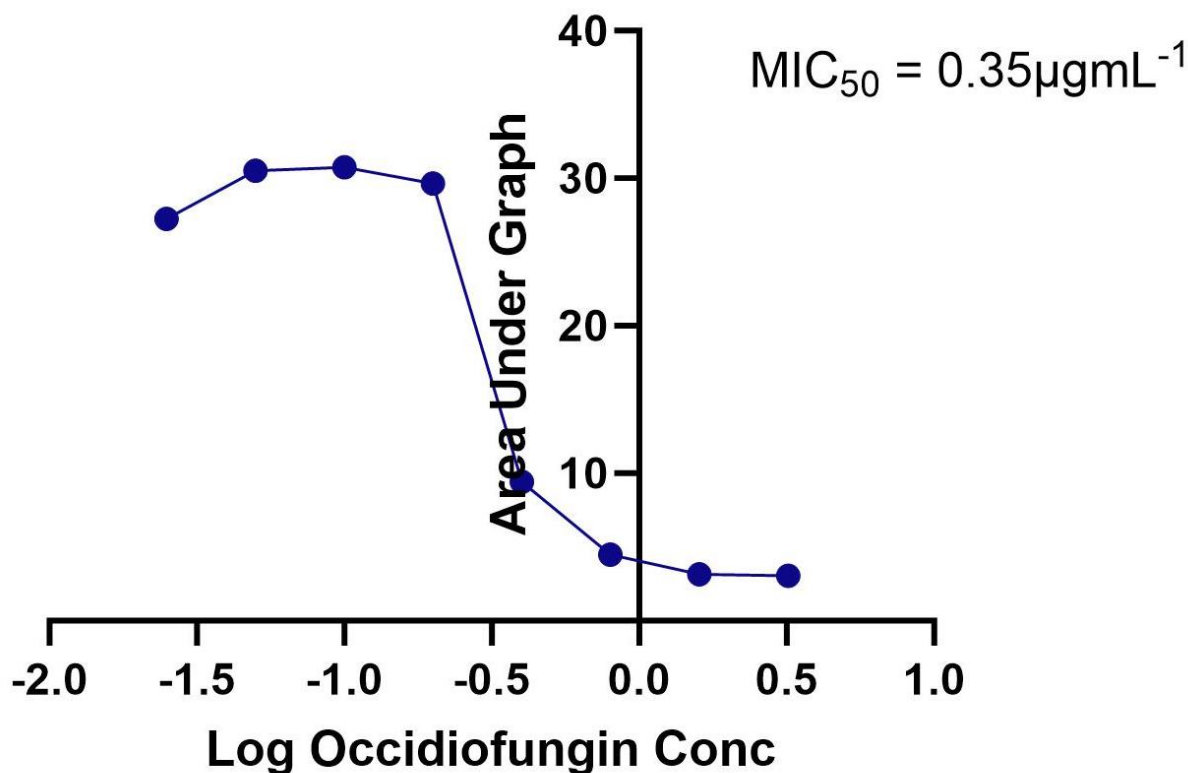


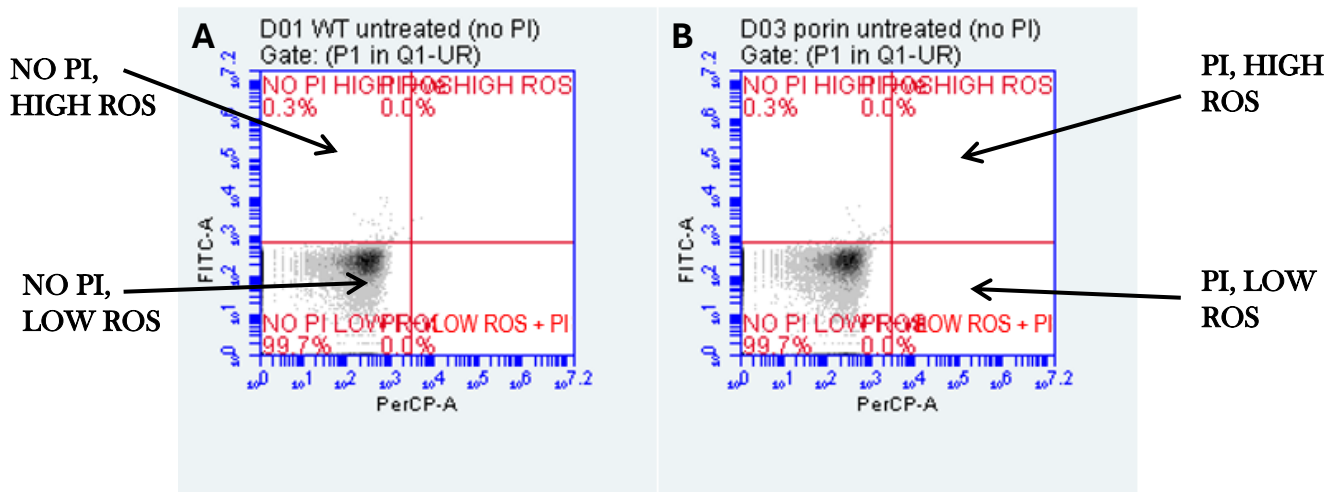
**Figure. 3.1.** Growth curve to show *Saccharomyces cerevisiae* cells treated with varying concentrations of Occidiofungin. Occidiofungin was serially diluted along columns 2-9, with each step representing a 2-fold dilution. This resulted in a final dilution of 128-fold in the last column. Starting concentration was 3.2 µgmL<sup>-1</sup>, columns 10 and 11 were used as controls, with a YPD control and an untreated control. Cells were grown overnight at 30°C in YPD, diluted and then added to the wells at a final OD of 0.1. The plates were then placed in a SpectroStarNano and grown for 24 hours at 30°C. The results were then used to make a line graph which was then placed into GraphPad for analysis of area under the curve and this was plotted on the X-axis and the Log of each Occidiofungin concentration on the Y-axis. The graph represents a single representative experiment.

### ***3.1.1 ROS accumulation and necrosis in Δpor1 cells when compared to Wild Type Saccharomyces cerevisiae using flow cytometry.***

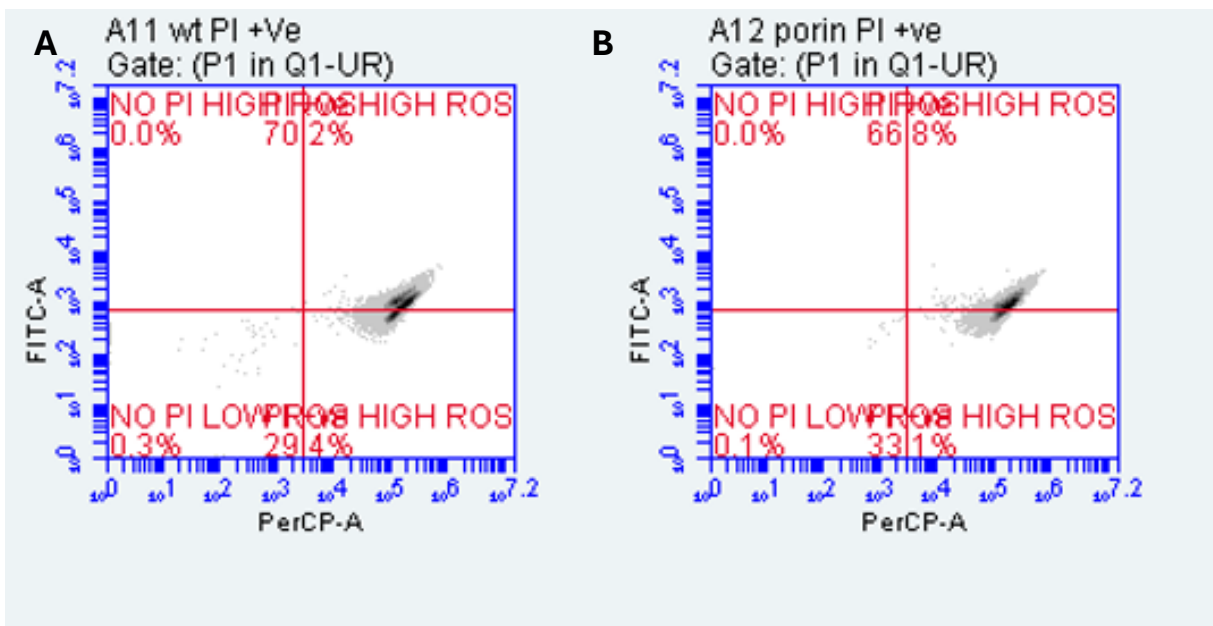
Data has been published that suggests Occidiofungin may stabilise the F-Actin cytoskeleton in yeast cells, which may account for its anti-fungal effects (44). In addition our lab has published evidence to suggest that stabilisation of Actin leads to an increase in cell death as a result of the inappropriate activation of MAPK cell integrity pathway (CWI) that is dependent on the outer mitochondrial membrane Voltage Dependent Anion Channel, Porin (43). To investigate

whether Porin 1 was required to mediate the antifungal effects of Occidiofungin we tested its efficacy in a porin deletion *S.cerevisiae* strain ( $\Delta por1$ ).

We measured the recognised cell death markers of ROS elevation and PI uptake in wild type and  $\Delta por1$ , both with and without Occidiofungin treatment ( $0.24\mu\text{g mL}^{-1}$  for 2 hours) using flow cytometry. Unstained samples were run to set a baseline value and showed the vast majority of cells (99.7%) in the bottom left quadrant, this was therefore representative of healthy living cells (Figure 3.2). A positive control for PI uptake indicating necrosis and fluorescence from the ROS indicator dye upon necrosis, was used by boiling *S.cerevisiae* cells for 15 minutes before the addition of stain to the sample (Figure 3.3). From the two graphs in Figure 3.3 we see that boiled necrotic cells showed a reproducible pattern, with the majority of the cells breaching the X-axis threshold value set from unstained controls (70.2% and 66.8% in the upper right quadrant, 29.4% and 33.1% in the lower right quadrant for Wt and  $\Delta por1$  cells respectively). The graphs also showed that the necrotic cells also displayed an increased level of ROS signal after the 15 minute boiling period, with around 2/3s of the total cells presenting above the Y-axis threshold. Figure 3.4 shows the PI and ROS staining result for the Wt and  $\Delta por1$  cells after treatment with  $0.24\mu\text{g mL}^{-1}$  Occidiofungin for a 1 hour period. Both cell types displayed similar quadrant percentages (lower left quadrant - 30.2% and 33.8%, lower right quadrant - 15.3% and 13.6%, upper right quadrant - 22.0% and 27.3%, upper left quadrant - 32.4% and 25.2%, for Wt and  $\Delta por1$  cells respectively). The quadrant values were not statistically different between Wt and  $\Delta por1$  following Occidiofungin treatment, indicating that they had the same response to drug treatment (Table 3.1).

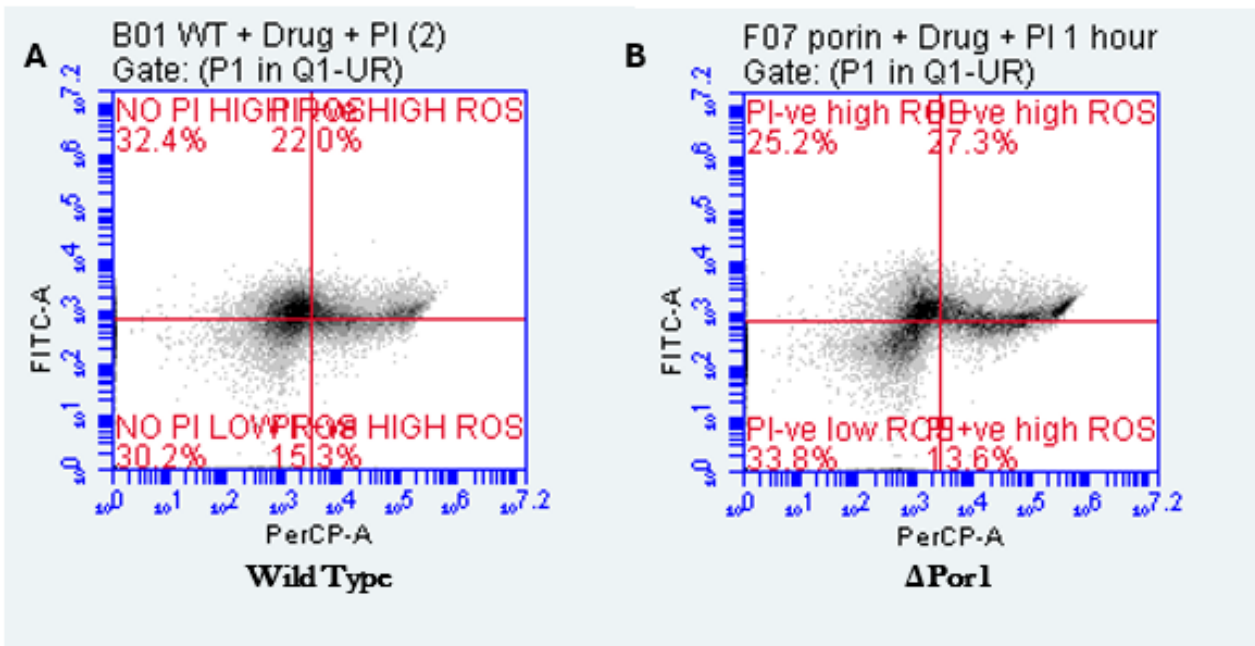


**Figure 3.2.** Cell type classification in conjunction with H2DCF-DA and PI signal characteristics. A positive control group of untreated cells were grown to log phase in YPD media without addition of PI. Cells below the y-axis threshold were classified as Low ROS, whilst those that breached the x-axis threshold were perceived as necrotic. Live cells (non-necrotic) are measured through the proportion of cells occupying the lower quadrants. Each Quadrant condition is labelled above. A - Wt. B -  $\Delta por1$ .



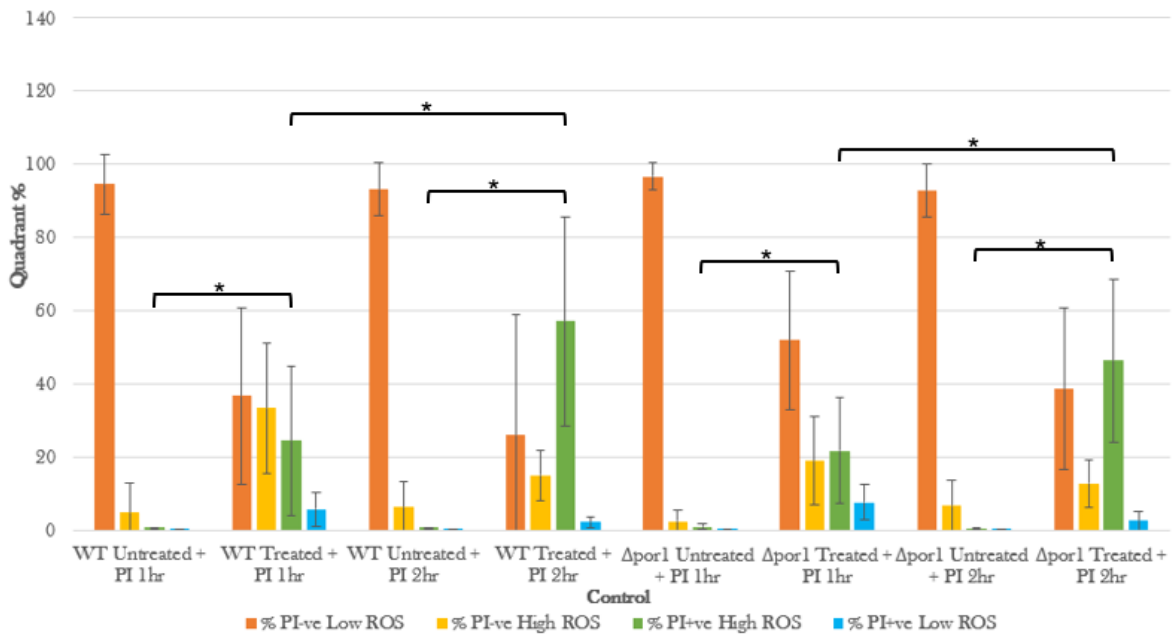
**Figure 3.3.** Plots to show the heat treated positive controls of both cell types, this shows the profile of fully necrotic cells that were heated to 100 °C for 15 minutes. These samples were then run through the flow cytometer to give the graph profiling seen above. A - Wt. B -  $\Delta por1$ .

Figure 3.3 displays that under typical necrosis, the cells presented with a ROS that was in between the threshold and the majority of cells also displayed a positive for Propidium Iodide.



**Figure 3.4.** Graphs to display the cell classifications after 60 minutes treatment of Occidiofungin at a concentration of  $0.24\mu\text{g mL}^{-1}$  in both Wt and  $\Delta\text{por1}$  *S.cerevisiae* cells. Cells were grown overnight and then diluted to an OD of 0.1, these cells were then grown to log phase, after they reached log phase Occidiofungin was added and they were treated for 60 minutes at  $30^\circ\text{C}$ . The cells were then run through the flow cytometer. These graphs are used as a representative for 3 biological replicates that were conducted for these controls. A - Wt. B -  $\Delta\text{por1}$ .

When the two controls were compared in the Wt and  $\Delta\text{por1}$  the data showed that there was a significant difference in the number of necrotic and ROS positive cells when compared to the untreated control (Figure 3.5). This was also evident when the 1 hour treated samples were compared to the 2 hour treated samples.



**Figure 3.5.** Bar graph displaying the Quadrant percentages shown through the PI/H2DCF-DA staining results for  $\Delta por1$  and Wt cells treated with  $0.24\mu\text{g mL}^{-1}$  Occidiofungin. Each Condition represents the average from 3 biological repeats. The error bars represent the standard deviation between the biological repeats. The statistical significance was tested using a One-way ANOVA test. Statistical significance is represented via the bars with asterisks, these bars represent quadrants that are significantly different from each other (P value < 0.05).

**Table 3.1.** Table to show the P-value from t-Test: Two-Sample Assuming Equal Variance that was carried out on select controls. This was to assess whether there was a significant difference in the percentages of each separate quadrant. It also analysed whether the quadrant values of the Wt and *Δpor1* cells were significantly different under treatment of Occidiofungin. P<0.05.

Compared Controls	Quadrant	P-value
Wt untreated + PI (1hr)/Wt treated + PI (1hr)	% PI+ve High ROS	0.001
Wt untreated + PI (2hr)/Wt treated + PI (2hr)	% PI+ve High ROS	0.025
Wt treated + PI (1hr)/Wt treated + PI (2hr)	% PI+ve High ROS	0.013
<i>Δpor1</i> untreated + PI (1hr)/ <i>Δpor1</i> treated + PI (1hr)	% PI+ve High ROS	0.004
<i>Δpor1</i> untreated + PI (2hr)/ <i>Δpor1</i> treated + PI (2hr)	% PI+ve High ROS	0.022
<i>Δpor1</i> treated + PI (1hr)/ <i>Δpor1</i> treated + PI (2hr)	% PI+ve High ROS	0.049
Wt treated + PI (1hr)/ <i>Δpor1</i> treated + PI (1 hr)	% PI-ve Low ROS	0.246
	% PI-ve High ROS	0.126
	% PI+ve High ROS	0.794
	% PI+ve Low ROS	0.490
Wt treated + PI (2hr)/ <i>Δpor1</i> treated + PI (2 hr)	% PI-ve Low ROS	0.675
	% PI-ve High ROS	0.756
	% PI+ve High ROS	0.696
	% PI+ve Low ROS	0.887

### 3.1.2. Necrosis Assay to determine the death time course of *S.cerevisiae* cells upon Occidiofungin treatment.

As we had determined that Occidiofungin treatment led to an increase in necrosis, a time lapse experiment was conducted to establish the rate of cell death within a culture. Figure 3.6 shows that 50% of *S.cerevisiae* cells were necrotised by Occidiofungin after around 90 minutes of treatment. Occidiofungin treatment led to a linear increase in cell death after 30 minutes, while untreated cells displayed negligible necrosis even after two hours. After two hours of Occidiofungin treatment time at a concentration of  $0.35\mu\text{g mL}^{-1}$  we observed necrosis in 80% of the cell population as indicated by PI uptake.

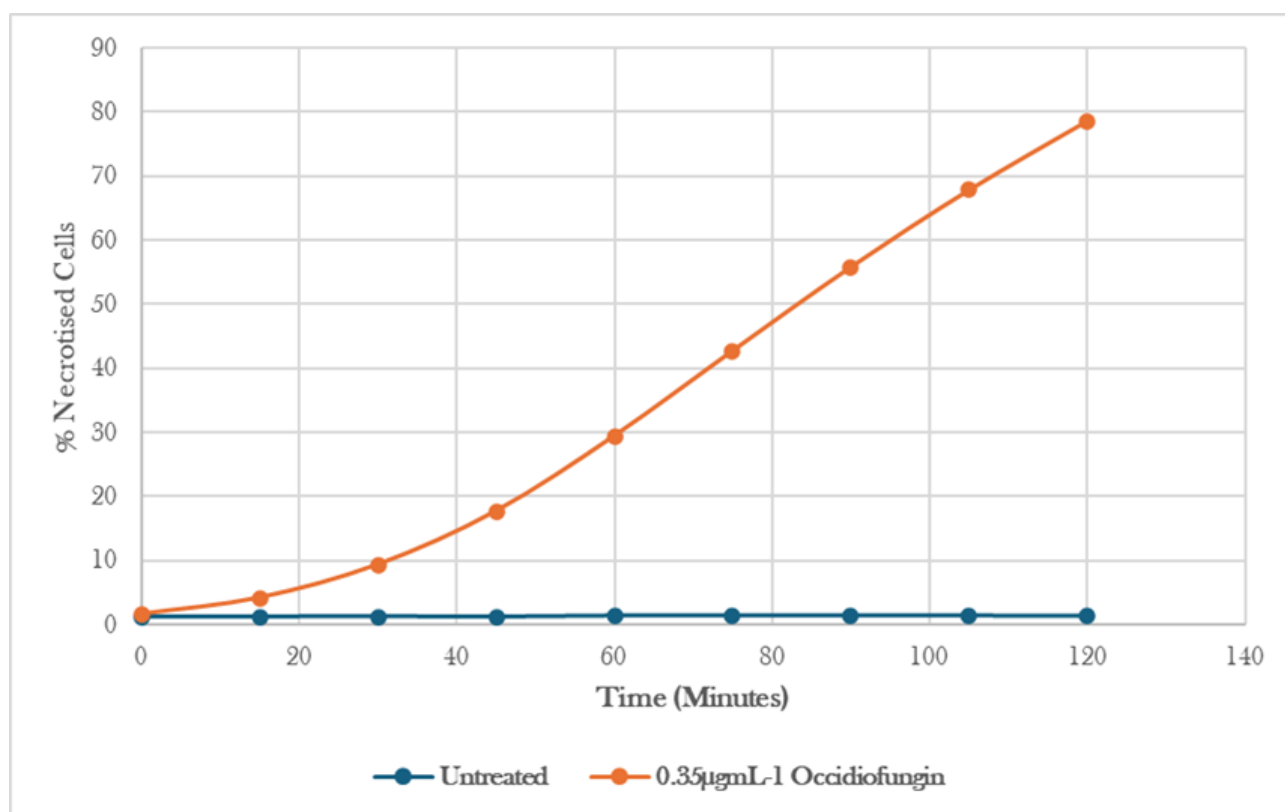


**Figure 3.6.** Graph to show the necrosis of Log phase *S.cerevisiae* cells treated with  $0.35\mu\text{g mL}^{-1}$  Occidiofungin compared with cells that remained untreated at  $30^{\circ}\text{C}$ . PI was added at  $10\mu\text{g/mL}$  prior to running samples through a flow cytometer at 15 minute intervals to show the percentage of cells necrotised at each timepoint, over a 2 hour treatment period. This graph is a single representative experiment, with no technical replicates.

### ***3.1.3 Use of Fluorescence microscopy to examine the effects of Occidiofungin treatment on lipid droplet formation in wild type and $\Delta por1$ cells.***

Lipid droplets serve as storage organelles for neutral lipids within yeast cells, playing a critical role in energy homeostasis within the cell. Porin 1 is essential in maintaining mitochondrial function and mitochondria are crucial to regulate lipid metabolism. Previous published data showed that Actin stabilisation led to an increase in lipid droplet accumulation that was dependent on Porin 1 presence (43). As changes in lipid homeostasis can result in loss of membrane stability and loss of viability we wished to determine if Occidiofungin treatment led to a Porin dependent change in lipid droplet number. To achieve this we made use of the neutral lipid stain Bodipy 493/503. Under the widefield microscopy the dye emitted bright green fluorescence, this allowed for clear visualization of lipid droplets within the cells. The cells were sampled after 1 hour and 2 hours of treatment with  $0.24\mu\text{g mL}^{-1}$  Occidiofungin. The samples were placed in a  $30^{\circ}\text{C}$  incubator during the 2 hour treatment window.

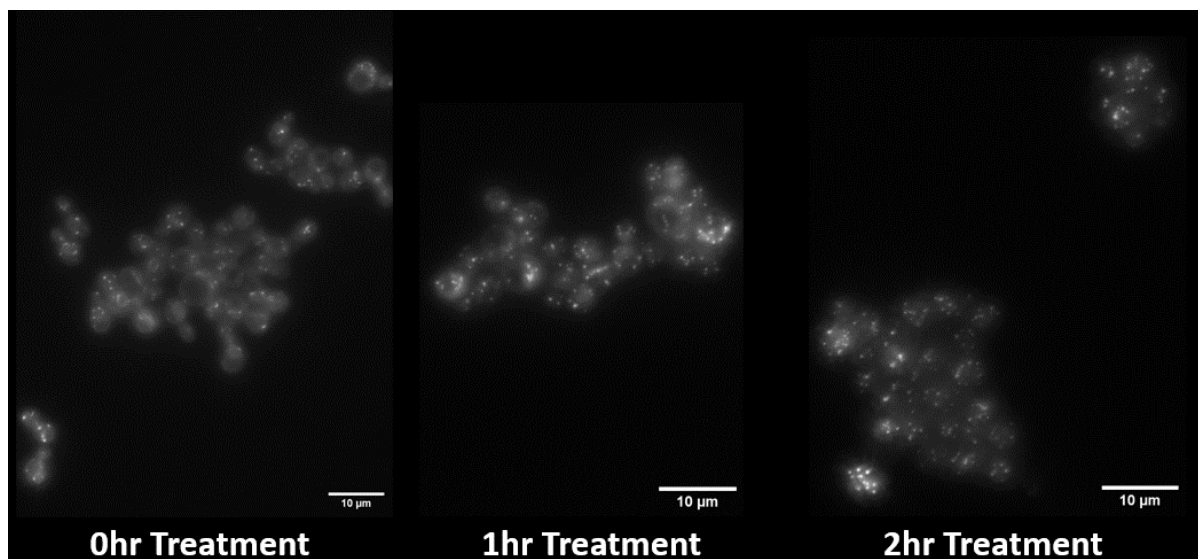


**Figure 3.7.** Image to show lipid droplets (white dots) present in Wt *S.cerevisiae* cells grown to log phase and then treated with  $0.24\mu\text{g mL}^{-1}$  Occidiofungin for a 2 hour time period. Displaying the effects of the treatment in 1 hour increments. Cells were stained with Bodipy 493/503. Images were gathered using an Olympus IX81 fluorescence microscope, with GFP 395/509 nm excitation/emission, at 100x magnification, using an Andor Xyla 4.2 CMOS digital camera.

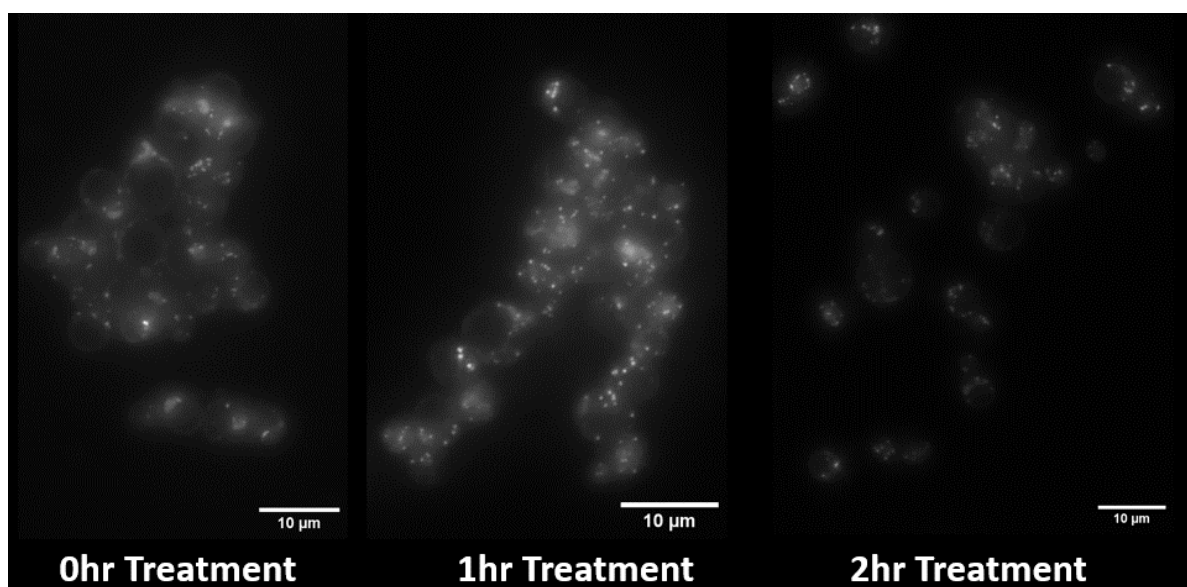


**Figure 3.8.** Image to show lipid droplets (white dots) present in  $\Delta por1$  *S.cerevisiae* cells grown to log phase and then treated with  $0.24\mu\text{g mL}^{-1}$  Occidiofungin for a 2 hour time period. Displaying the effects of the treatment in 1 hour increments. Cells were stained with Bodipy 493/503. Images were gathered using an Olympus IX81 fluorescence microscope, with GFP 395/509 nm excitation/emission, at 100x magnification, using an Andor Xyla 4.2 CMOS digital camera.

**Table 3.2.** Table to show the average lipid droplet count per cell in both the Wt and  $\Delta por1$  cells, each average was taken from a minimum of 18 cells and are representative of the two Figures 3.8 and 3.7 as a single experimentation without repeats. The percentage difference between the lipid droplet counts of the two cell types was calculated and displayed above.

	Lipid Droplets Per cell (AVG)		
	0hr	1hr	2hr
Wt	4.28	8.04	9.13
$\Delta por1$	2.93	5.55	6.28
% difference	68.50	69.02	68.77

The percentage difference in the average lipid droplet counts per cell remained between 68.5% and 69.1% during its 2 hour treatment period with Occidiofungin (Table 3.2). The  $\Delta por1$  cells contained less lipid droplets overall, in line with the published observations that *Por1* plays a role in lipid storage, however the addition of Occidiofungin increased the number of these lipid droplets in a manner that was relative to the increase seen in the Wt cells.

### ***3.2 Ascertaining whether Actin is a target of Occidiofungin.***

It has been proposed that Actin may represent the target of Occidiofungin (34). As Actin is required for membrane stability this may represent a reasonable explanation for the increase in necrosis we observe upon treatment. Although our data did not suggest that recognised downstream effects of Actin stabilisation (Porin dependent MAPK CWI activation and lipid storage) played a role in the mode of action of Occidiofungin, we wished to explore the effects of Occidiofungin on Actin further. We used a variety of different experimentation techniques to assess if Occidiofungin treatment had measurable effects on the cell that could be linked to Actin stabilisation.

#### ***3.2.1. Analysing a library of Actin mutant strains to assess a synthetic interaction with Occidiofungin.***

It has been suggested that Occidiofungin may bind Actin (34), if this were the case we may expect to observe a synthetic interaction between the drug and strains expressing mutated forms of Actin. As an example, changes in the surface charge of Actin, introduced by mutation, may increase or decrease Occidiofungin binding and so lead to sensitivity or resistance. We made use of an isogenic library of Actin mutants in which a number of charged residues have been replaced by alanine (45). We then tested whether we could observe changes in Occidiofungin efficacy.

Actin mutant act1-111 was the only mutant strain that did not show a statistically significant decrease in growth when compared to the Wt strain (Table 3.3). The act1-111 mutant strain has been shown to inhibit the interaction between Actin and the Actin nucleating protein Las17 (51). This therefore indicated the potential for Actin to be a target of Occidiofungin, and therefore more experimentation on Actin was required.

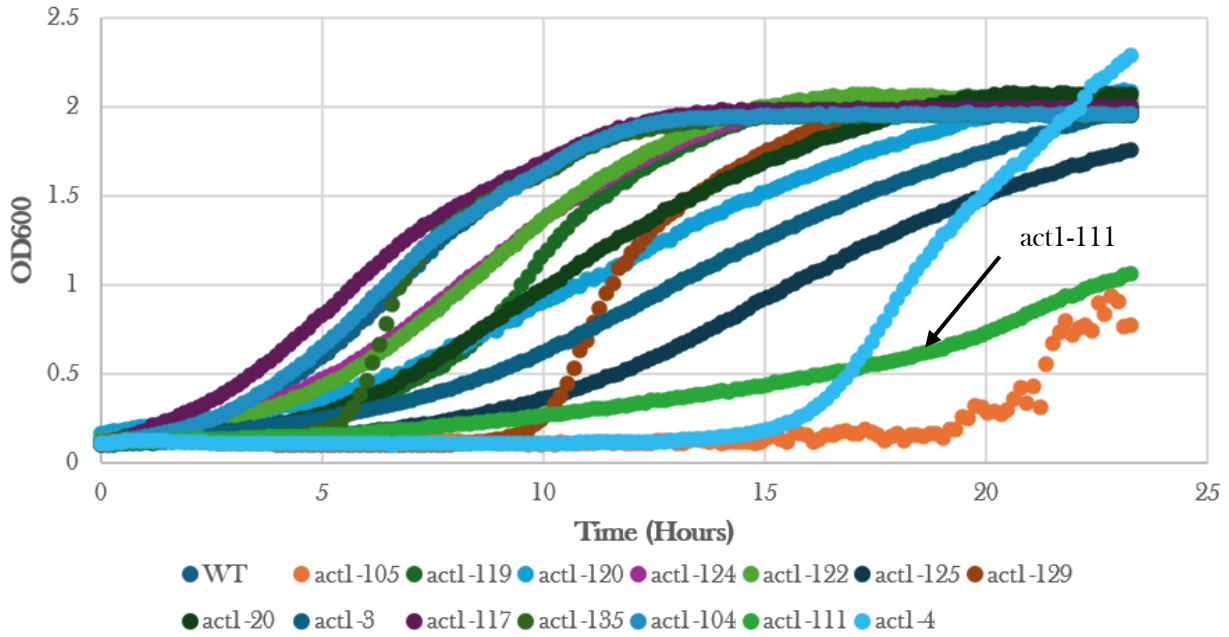


**Figure 3.9.** Graph to show the normal growth of the *S.cerevisiae* Wt and different Actin mutant strains, at 37°C in a 24 hour time period. A SpectroStarNano Plate reader was used to record this. Each point on the graph represents an average from 3 technical replicates.

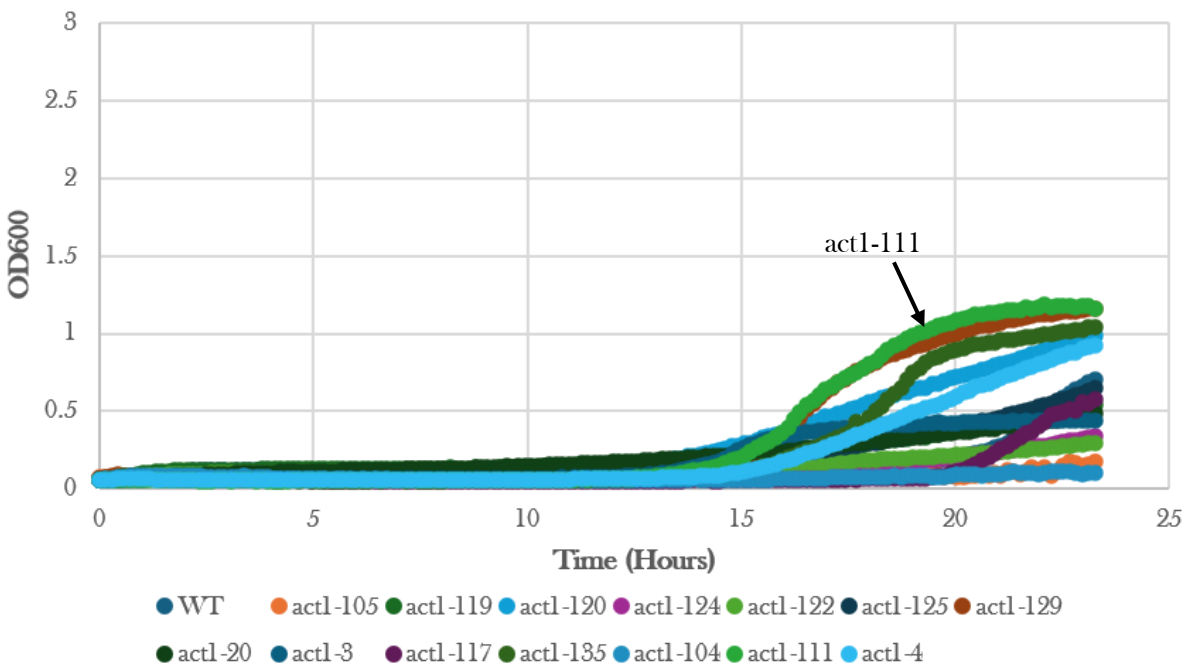


**Figure 3.10.** Graph to show growth *S.cerevisiae* Wt and different Actin mutant strains when treated with 0.35µgmL<sup>-1</sup> Occidiofungin at 37°C in a 24 hour period. A SpectroStarNano Plate reader was used to record this. Each point on the graph represents an average from 3 technical replicates.

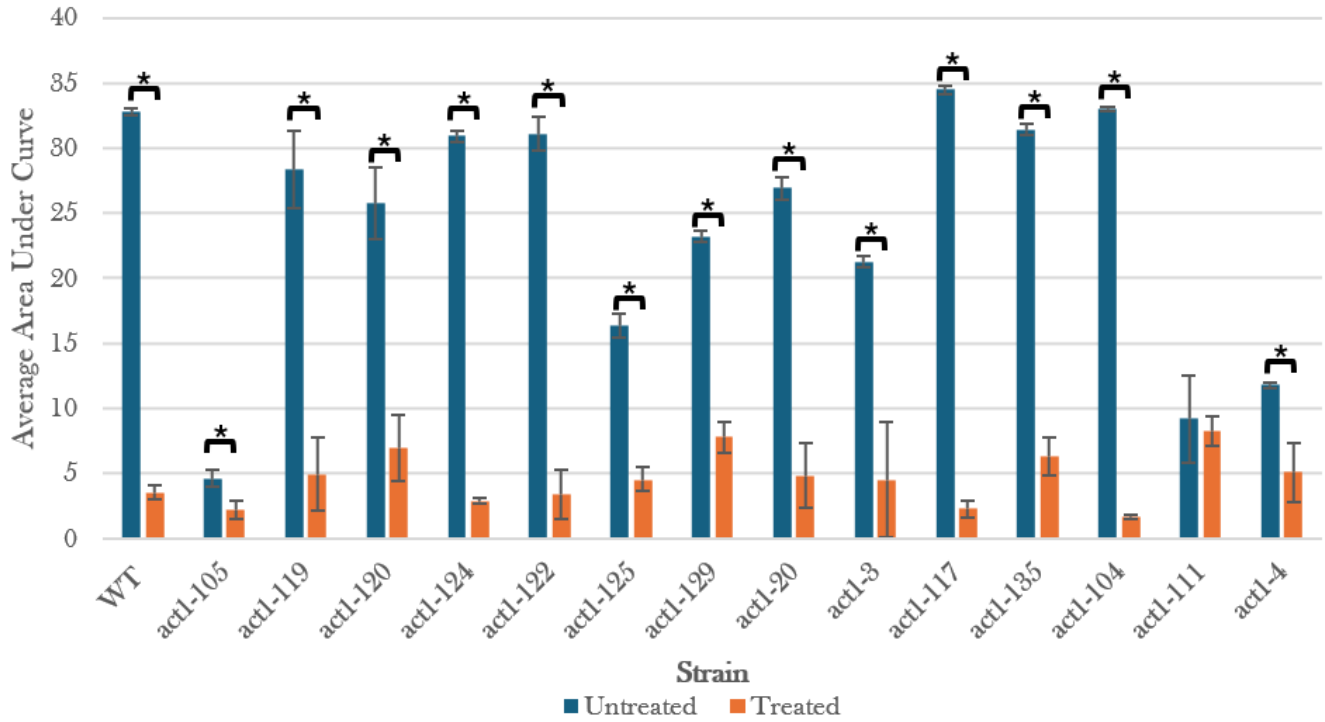


**Figure 3.11.** Bar graph to show the area under the curve from the untreated and treated Actin mutants. This graph was made using the two figures above. The error bars are representative of the standard deviation between 3 technical replicates at each control. The statistical test carried out was a 1 tail Paired distribution t-test; this was carried out using the 3 technical replicates at each control. Statistical significance is represented via the bars with asterixis, these bars represent quadrants that are significantly different from each other. P-value < 0.05.

**Table 3.3.** Table to show the area under the curve for each mutant strain in the treated and untreated assays in a 24 hour period. This table is representative of Figure 3.11. This table shows the Statistical significance of the different strains when the Occidiofungin treated controls are compared to the untreated controls. This was done using the average of 3 technical repeats for the area under the curve. The statistical test carried out was a 1 tail Paired distribution t-test, this was carried out using the 3 technical replicates at each control.  $P < 0.05$ .

	Average Area Under the Curve		P-Value
	Untreated	Treated	
<b>Wt</b>	32.79	3.54	0.00
<b>act1-105</b>	4.61	2.22	0.02
<b>act1-119</b>	28.37	4.94	0.01
<b>act1-120</b>	25.74	6.94	0.01
<b>act1-124</b>	30.93	2.90	0.00
<b>act1-122</b>	31.11	3.39	0.00
<b>act1-125</b>	16.35	4.53	0.01
<b>act1-129</b>	23.22	7.78	0.00
<b>act1-20</b>	26.91	4.81	0.01
<b>act1-3</b>	21.28	4.51	0.02
<b>act1-117</b>	34.48	2.26	0.00
<b>act1-135</b>	31.43	6.27	0.00
<b>act1-104</b>	33.01	1.66	0.00
<b>act1-111</b>	9.19	8.20	0.39
<b>act1-4</b>	11.81	5.08	0.02

Table 3.3 displayed that *act-1-111* was the only mutant strain that did not display a statistically significant difference to its normal growth, when treated with Occidiofungin. This could be due to the strain showing very poor growth at the untreated control.

### 3.2.2 Using GFP tagged ABP-1 to assess the effect Occidiofungin has cortical Actin patch dynamics using fluorescence microscopy.

To investigate whether Occidiofungin had a direct effect on Actin structures within a yeast cells we introduced a plasmid expressing a GFP tagged version of the Actin binding protein ABP1, which localises to cortical Actin patches. This enabled us to visualise the effects of Occidiofungin in real time using fluorescence microscopy (Figure 3.12).

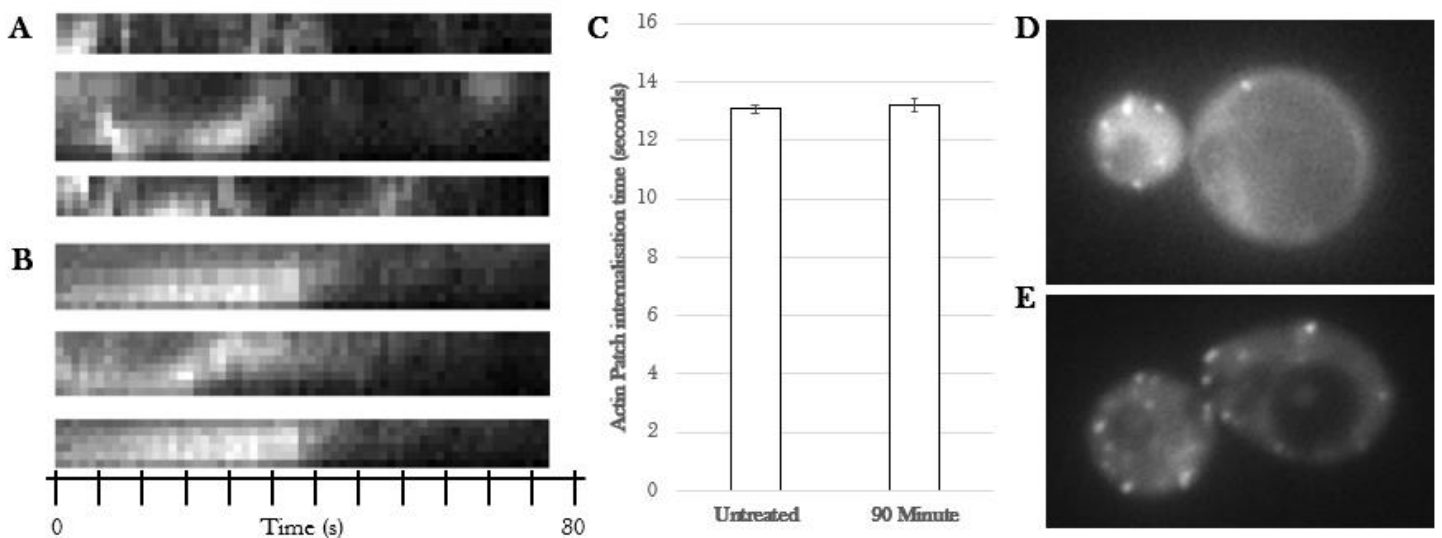


**Figure 3.12.** **A** - displays 3 kymographs that are representative of 3 different loci to on an untreated *Saccharomyces cerevisiae* cell, they represent the time taken for an Actin patch to endocytose within the cell and subsequently disappear from view under the microscope. These were taken from a 2 minute timelapse using a widefield microscope. **B** - displays kymographs for *Saccharomyces cerevisiae* cells that have been treated for 90 minutes with  $0.35\mu\text{g mL}^{-1}$  Occidiofungin. These were taken from a 2 minute timelapse using the widefield microscope. **C** - displays a bar graph with the average time taken for an Actin patch to endocytose from the membrane of the *Saccharomyces cerevisiae* cell, with the error bars representative of the Standard deviation between each replicate. The x-axis shows the control that each bar represents. **D** - Image displaying the GFP-ABP1 Actin cortical patches in an *S.cerevisiae* cell that has not been treated with Occidiofungin. **E** - Image displaying the GFP-ABP1 Actin cortical patches in an *S.cerevisiae* cell that had been treated for 90 minutes with  $0.35\mu\text{g mL}^{-1}$  Occidiofungin. These values were calculated using a velocity measurement tool in ImageJ. The Kymographs were made using ImageJ. 3 samples were analysed for both untreated and treated controls.

Figure 3.12 shows that the average time for a cortical Actin patch to internalise within a cell.

The calculated P-value from a T-test was 0.127 and therefore the difference between the two readings was not significant. This suggested that even when treated with Occidiofungin the mean time for an Actin cortical patch to endocytose was unchanged and therefore suggested

that Actin was not a target of Occidiofungin. In addition visual inspection of cells treated with Occidiofungin suggested that Actin patch size and distribution was not altered, however it should be noted that a significant number of cells lost GFP fluorescence upon addition of Occidiofungin. It may therefore be the case that data represents the non-necrotic cell population still present after 90 minutes of Occidiofungin treatment.

### ***3.3 Haemolysis assay to assess whether Occidiofungin treatment leads to Red Blood Cell lysis.***

We have determined that Occidiofungin treatment leads to the destabilisation of yeast cell membranes and necrosis. We therefore wished to investigate whether a similar effect could be observed in mammalian cells. To investigate this we employed a Haemolysis assay using agar plates containing sheep blood. This allowed me to assess whether the application of Occidiofungin at varying concentrations would destabilise the plasma membrane of red blood cells resulting in their lysis (Figure 3.13). Occidiofungin was applied at 0.035, 0.35, 3.5 and 35  $\mu\text{g mL}^{-1}$ . A positive (10% SDS) and a negative ( $\text{H}_2\text{O}$ ) control were also used.

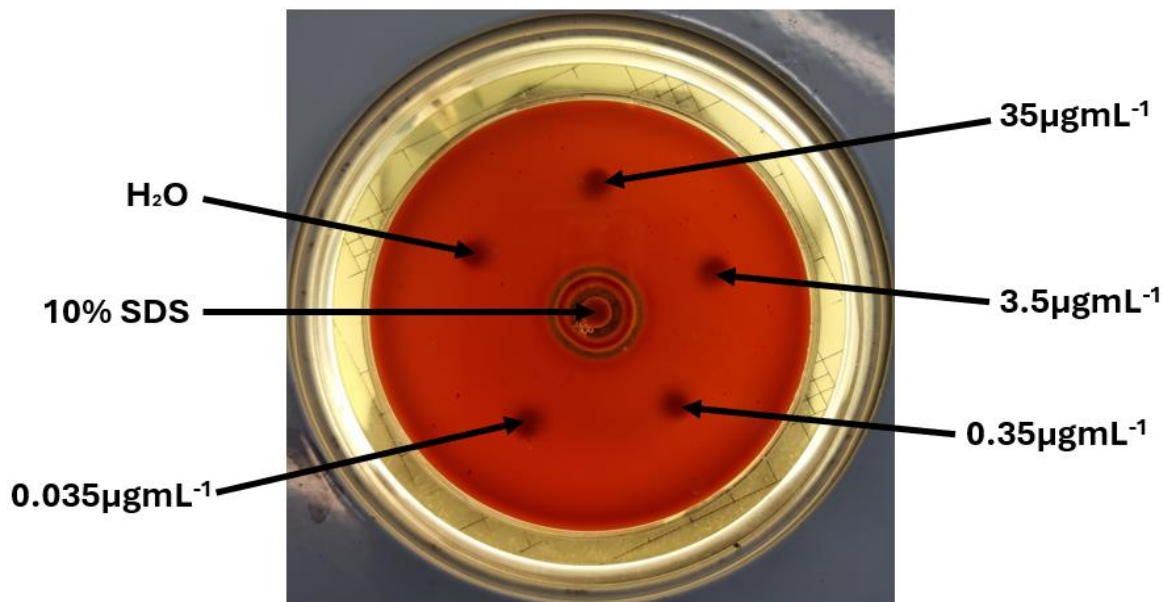


**Figure 3.13.** Picture of a blood agar plate after a 24 hour incubation at 37°C, 10% SDS used as a positive lysis control.  $\text{H}_2\text{O}$  was used as a negative control. The other four differing concentrations represent Occidiofungin. This was repeated on 4 identical plates, with each result displaying the same phenotype (Only the 10% SDS positive control led to the ring formation seen around the middle filter paper disc). This plate was representative for all repeats.

As expected a ring formation representing red blood cell lysis was observed around the SDS positive control. The Negative (H<sub>2</sub>O) control did not lead to the generation of a zone of lysis. As seen in Figure 3.12 even at a concentration that is 10 fold the MIC<sub>50</sub>, Occidiofungin displayed no lysis of the RBS's in this assay.

### ***3.3.1 Use of *Galleria mellonella* as an infection model to assess the efficacy and toxicity of Occidiofungin within a living system.***

*Galleria mellonella* can be used as an effective infection model as they possess an innate immune system with functional parallels to mammalian immunity (49). They are able to survive at 37°C, closely mimicking the human physiological temperature as well as being the same temperature used in previous experimentations with Occidiofungin and yeast cells. I therefore used *Galleria mellonella* to test whether Occidiofungin treatment could prevent infection of the human fungal pathogen *Candida albicans*. The effects of Occidiofungin on *Galleria* lifespan were also tested to examine toxicity.

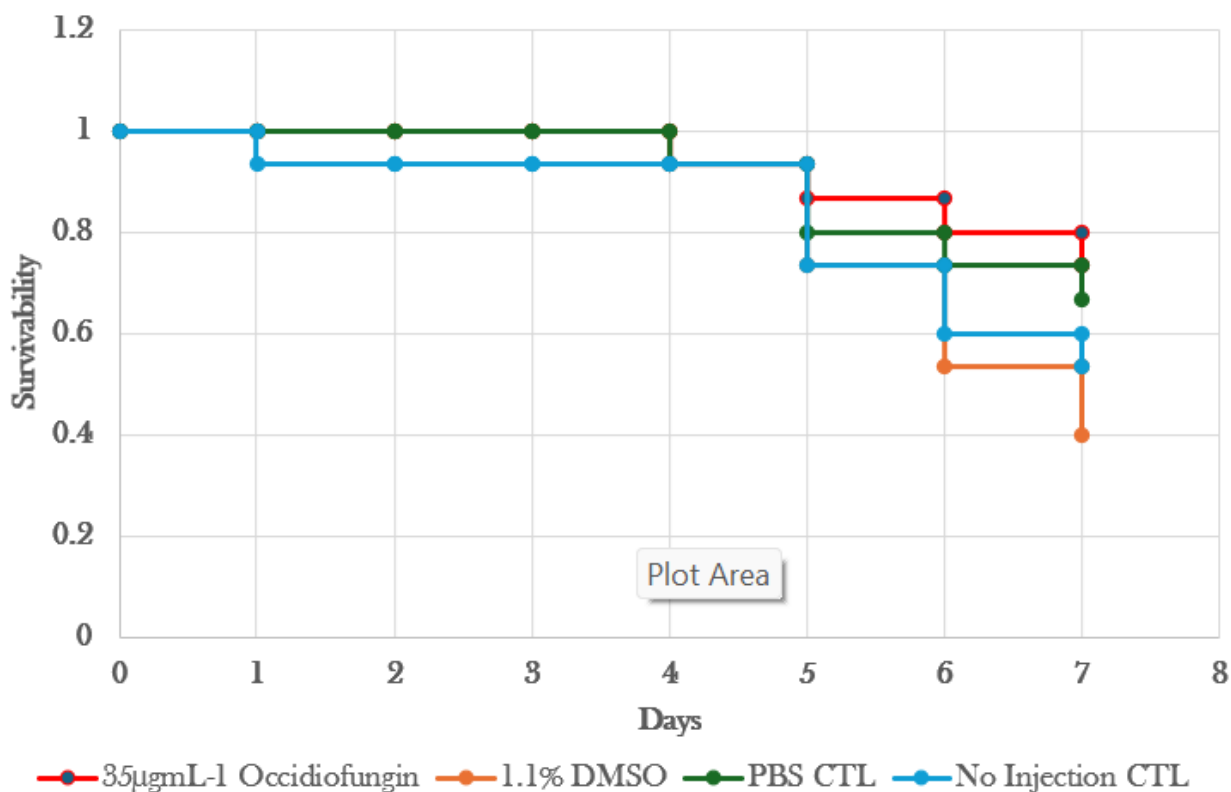


**Figure 3.14** Graph to show *Galleria mellonella* survivability assay over a 7 day period, testing the toxicity of 35µg mL<sup>-1</sup> Occidiofungin using 3 other controls, 1.1% DMSO, PBS and a Non injection control. Each larvae were kept at 37°C for the duration of the 7 days. Each worm was injected into their bottom left proleg, as well as selected at similar size and phenotype.

Figure 3.14 showed that a 100 fold increase in the concentration of Occidiofungin at the MIC had a similar effect on wax moth larvae survival when compared to the PBS and non-injection controls, with each losing viability of 25% and 30% after 7 days respectively. 1.1% DMSO treatment (solvent control) did have an effect on survival and resulted in a 60% loss in viability after the 7 day period, this was similar to the non-injected control. Overall these data suggest that loss in viability was not correlated with Occidiofungin treatment.

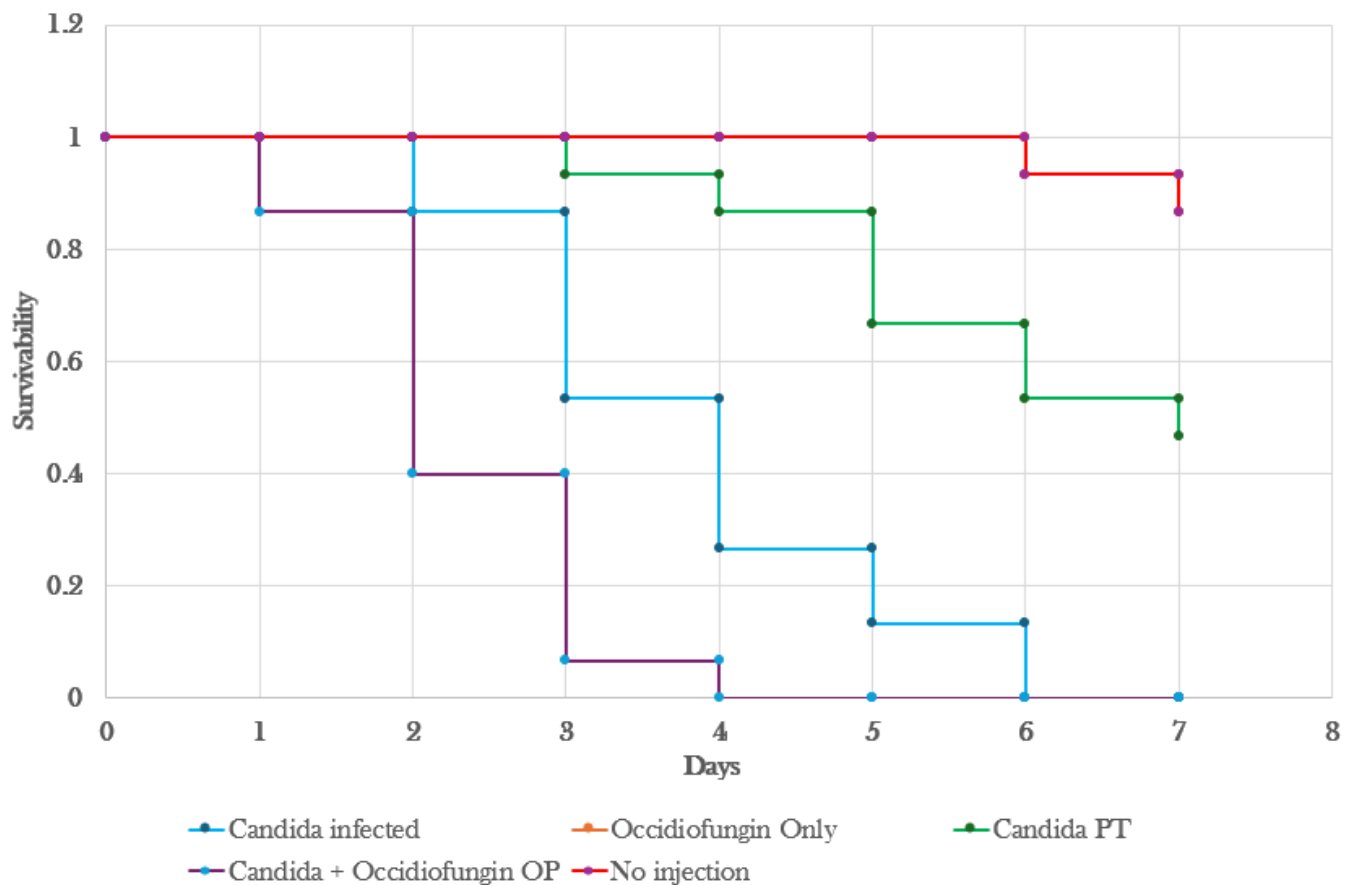


**Figure 3.15.** Survivability graph to display the survivability of 5 different *Galleria mellonella* controls. Each control contained 15 wax larvae; they were kept in an incubator at 37°C for the duration of the 7 day assay. All controls containing Occidiofungin used a concentration of 1.6µgmL<sup>-1</sup>. *Candida* PT - *Candida* that was pre-treated for 2 hours with Occidiofungin before it was injected into the larvae. *Candida* + Occidiofungin OP - *Candida albicans* and Occidiofungin were both injected but into separate pro legs.

*Candida albicans* infected larvae showed a poor survival rate with the entire population being dead after day 6 (figure 3.15). The Occidiofungin only control followed the exact same survival profile as the non-injection control, this is indicative that both these controls followed a common survivability profile of an untreated wax moth larvae. *C.albicans* that was pre-treated with Occidiofungin showed a survival profile that was indicative of a reduced infection when it is compared with the *Candida* infected control, this suggested that treatment with Occidiofungin reduced the number of viable cells and therefore this influenced the survivability of these larvae. The *Candida* and Occidiofungin opposite proleg injection control showed the worst survival rate, with the entire population being dead after day 4. This would suggest that

Occidiofungin is not able to decrease the pathogenicity of the *C.albicans* within the wax moth larvae when injected into an opposing proleg.

### ***3.3.2 Effects of Occidiofungin Treatment on Macrophage uptake of C. albicans cells.***

*C. albicans* cells are readily phagocytosed by macrophage cells upon recognition of pathogen associated molecular patterns (PAMPS) in the cell wall. As Occidiofungin treatment leads to necrosis, we wished to test whether Occidiofungin treatment has an effect on macrophage recognition and internalisation of *C. albicans* cells using an engulfment assay. *C. albicans* cells were treated with  $0.35\mu\text{g mL}^{-1}$  Occidiofungin for 1 hour, with a known number of cells introduced to  $1 \times 10^5$  macrophages and left for 4 hours at  $37^\circ\text{C}$ . These cells were then viewed under the widefield microscope and assessed for *C. albicans* uptake.

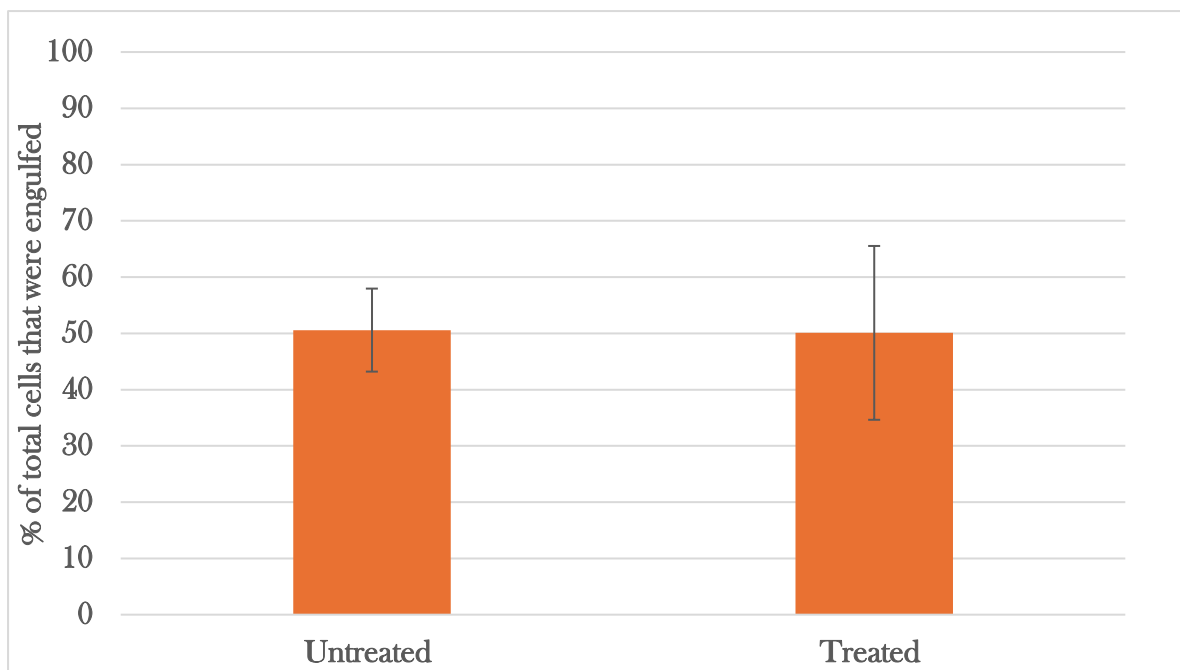


**Figure 3.16.** Bar graph to show the average percentage of the total number of cells that were up took by the macrophages in the macrophage engulfment assay. These values were calculated using 4 images at each control, with the cell numbers counted by eye. The averages were calculated from those values. The error bars represent the standard deviation between the % engulfed values for each control. The statistical significance was tested using t-Test: Two-Sample Assuming Equal Variance data analysis tool in excel, the calculated P- value was 0.86 which implied that the % of total cells that were engulfed by macrophages in the untreated and treated controls was not statistically different.

From Figure 3.16. we can see that the uptake of *C. albicans* was similar for untreated and Occidiofungin treated samples, suggesting that there was no increase in cell uptake. This was confirmed through statistical analysis using a t-Test: Two-Sample Assuming Equal Variance, which showed a P-value of 0.86.

### ***3.3.3 Assessment of the effects of Occidiofungin treatment on C. albicans biofilm formation.***

Our data suggest that Occidiofungin can kill yeast cells, including the human fungal pathogen *C. albicans*. As *C. albicans* forms biofilms that display elevated drug resistance we wished to determine whether the addition of Occidiofungin could inhibit biofilm growth and formation. This was done using XTT, which is a colorimetric method used to assess cell viability and

proliferation. This relies on the reduction of the tetrazolium salt XTT to an orange formazan dye by metabolically active cells. The formazan that is produced, is then able to be measured using a spectrophotometer and this then correlates with number of viable cells still remaining within the biofilm.

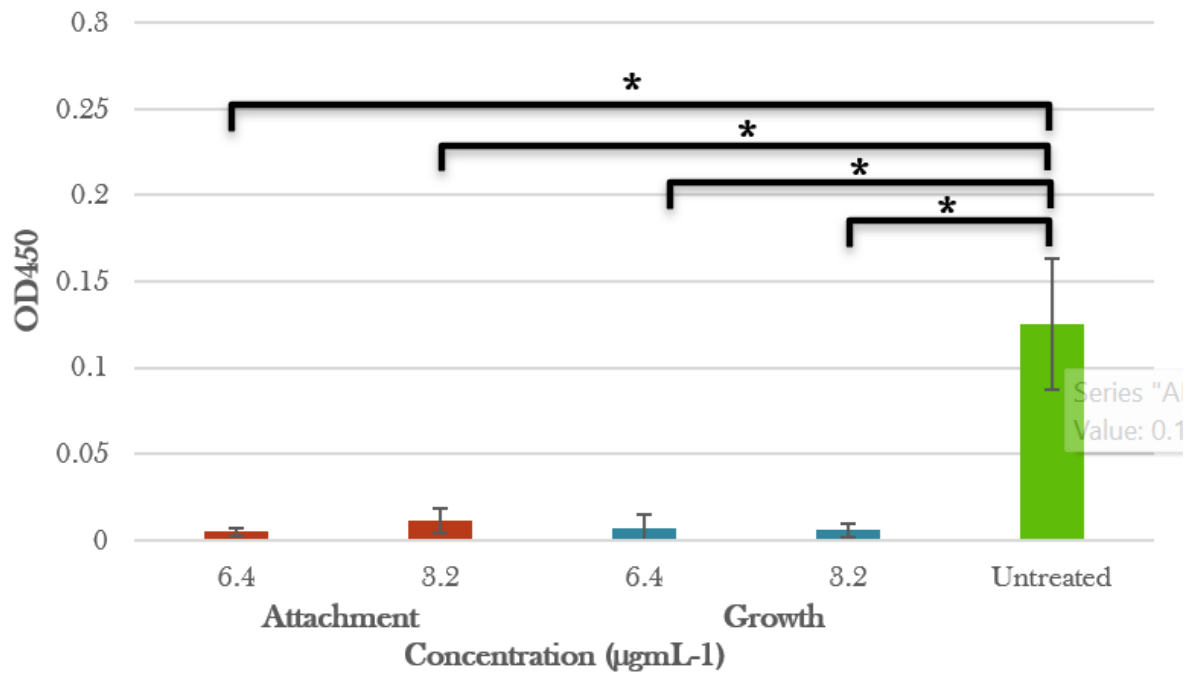


**Figure 3.17.** Graph to show *Candida albicans* SN250 biofilm maturation after 24 hours incubation at 37°C. An untreated growth control was tested in addition to samples that introduced Occidiofungin at growth and attachment stages using 2 separate concentrations (6.4µg mL<sup>-1</sup> and 3.2µg mL<sup>-1</sup>). The error bars representing the standard deviation between the 12 technical replicates for each concentration. Carried out on a 96 well plate and OD measured using a SpectroStarNano plate reader. The statistical significance was tested using a One-way ANOVA test. Statistical significance is represented via the bars with asterixis, these bars represent Controls that are significantly different from each other (P value < 0.05).

The addition of 6.4 and 3.2µg mL<sup>-1</sup> Occidiofungin at both the growth and attachment phases (refer to conducting a biofilm assay in methods for how this was done) of biofilm maturation led to a statistically significant inhibition of biofilm maturation when compared to the untreated control, this suggested that Occidiofungin was able to prevent biofilm formation.

### 3.4 Testing Occidiofungin against a variety *Candida* species

To investigate the efficacy of Occidiofungin to necrotise different *Candida* species we employed a Necrosis assay, where different strains were grown to log phase and then treated with Occidiofungin for 90 minutes, these samples were stained with Propidium Iodide and then run through a flow cytometer. Figure 3.18. displays that Occidiofungin is effective at killing multiple species of *Candida* in a short period of time. *Candida parapsilosis* displayed a 60% necrosis at  $1.6 \mu\text{g mL}^{-1}$  Occidiofungin treatment and around a 50% necrosis at  $0.8 \mu\text{g mL}^{-1}$  Occidiofungin treatment. *Candida tropicalis* displayed a 70% and around 60% necrosis at  $3.2$  and  $1.6 \mu\text{g mL}^{-1}$  Occidiofungin treatment respectively. *Candida dubliniensis* displayed around a 30% and 40% necrosis at  $3.2$  and  $1.6 \mu\text{g mL}^{-1}$  Occidiofungin treatment respectively. *Candida glabrata* displayed around a 90% necrosis at both the  $3.2$  and  $1.6 \mu\text{g mL}^{-1}$  Occidiofungin treatments. Even at the lower end of the scale there is still a 20% necrosis after 90 minutes.

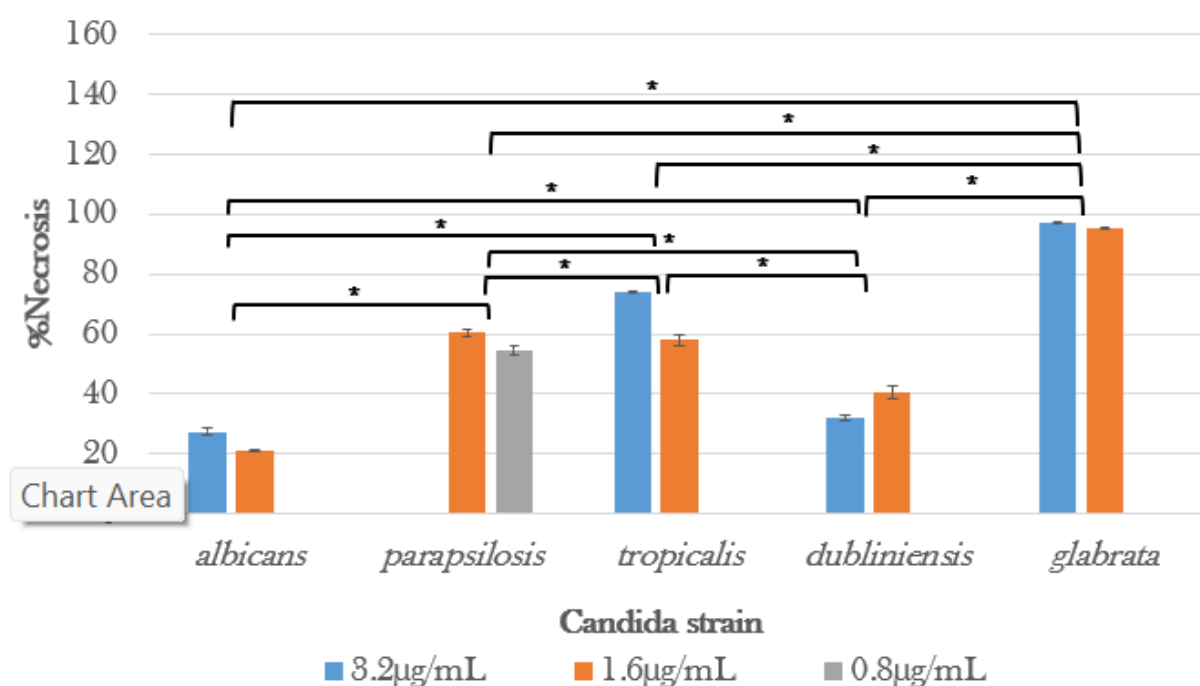


**Figure 3.18.** Graph to show the %Necrosis of different *Candida* species after 90 minutes of treatment at  $37^{\circ}\text{C}$  with Occidiofungin at  $3.2$ ,  $1.6$  and  $0.8 \mu\text{g mL}^{-1}$ . Each bar is representative of the average from 3 technical repeats. The statistical significance was tested using a Two-way ANOVA. Statistical significance is represented via the bars with asterix, these bars represent Controls that are significantly different from each other ( $P$  value  $< 0.05$ ).

### 3.5. Using an Alkyne derivatised Occidiofungin to examine Occidiofungin localisation

Occidiofungin is chemically modified with a terminal alkyne through acylation of the free amino group of the diaminobutyric acid residue at position 5, then derivatization with azide Alexa Fluor 488 installs a fluorescent tag on the drug, and this then forms Alkyne Occidiofungin (44). The introduction of this tag allowed for real time visualisation of Occidiofungin localisation using a fluorescent microscope.

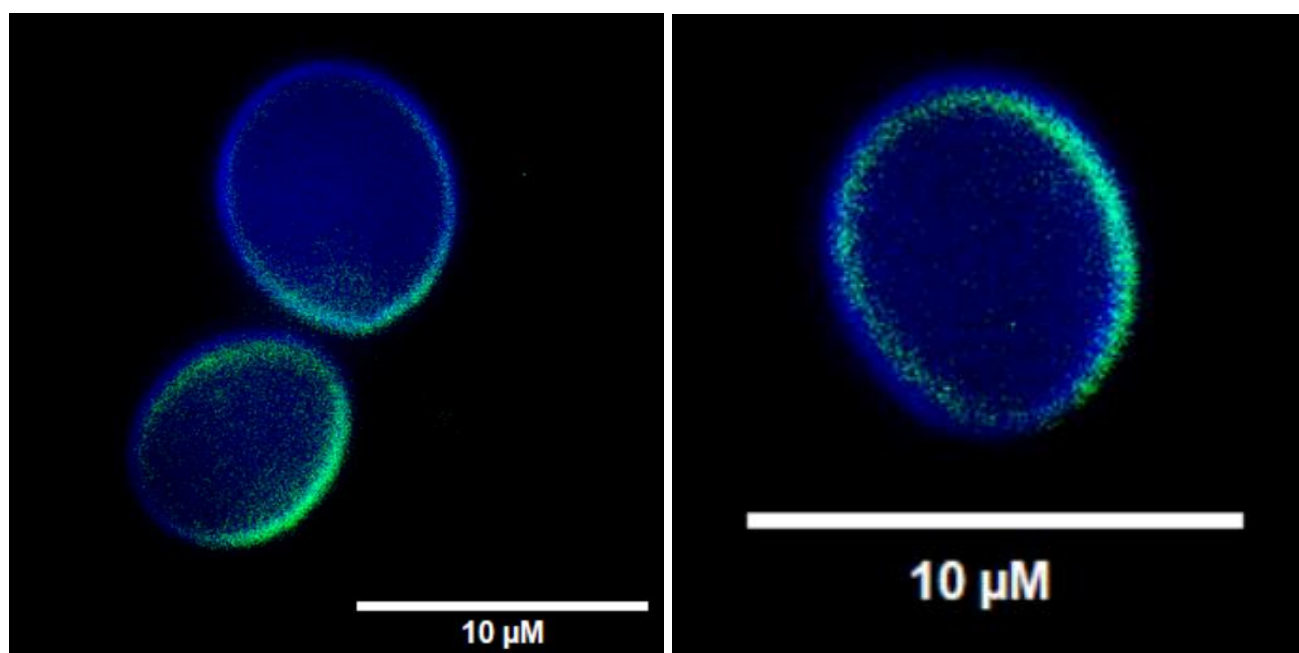


**Figure 3.19.** Microscopy images to show Alkyne Occidiofungin (Green colour) and 0.1% Calcofluor White stain (Blue colour) on *Candida albicans* cells that had been treated with  $0.4\mu\text{g mL}^{-1}$  Alkyne Occidiofungin for 50 minutes. Cells were grown overnight in YPD media, the cells were then diluted to a 0.1 OD and grow to log phase. Cells were then treated with Alkyne Occidiofungin for 50 minutes. Images were gathered using an Olympus IX81 fluorescence microscope, with GFP 395/509 nm excitation/emission, at 100x magnification, using an Andor Xyla 4.2 CMOS digital camera.

Figure 3.19 appears to show that alkyne Occidiofungin outlines the Calcofluor White stain. As Calcofluor White is a cell wall stain, this suggested that Occidiofungin targets the cells through attaching to either to cell wall or plasma membrane. Figure 3.19 also displays no internal staining of the cells, further indicating an outer cell target.

## 4. Discussion

The aim of this study was to investigate the mechanism of action of Occidiofungin as an antifungal. I investigated the current hypothesis that Actin may be target for Occidiofungin and that this may provide a mechanism for its action. I was able to reproduce the strong antifungal effect described for Occidiofungin which was in several yeast fungal pathogens and the model *S. cerevisiae*. My data demonstrated clearly that Occidiofungin is fungal specific and induces rapid necrosis in yeast cells and that this mode of cell death is consistent across pathogenic and non-pathogenic yeasts tested

### *4.1 Actin as a target for Occidiofungin*

Although some in vitro evidence exists that Occidiofungin has a weak binding affinity for Actin (34) little had been done to test its effects in living cells. To investigate this I employed a range of techniques that probed the direct effects on processes that require Actin.

The stabilisation of Actin has been shown to lead to cell death (43), this stabilisation can happen as a result of the inappropriate activation of the MAPK cell integrity pathway and this inappropriate activation is dependent on the outer membrane mitochondrial membrane Voltage Dependent Anion Channel which is Porin 1 (43). Therefore in order to test if this Actin /MAPK/Porin pathway was responsible for Occidiofungin inducing necrosis, a Por1 deletion strain was employed. Firstly through the use of a cell death assay in which the cell death markers Propidium Iodide (necrosis) and H<sub>2</sub>DCFDA (2',7'-dichlorodihydrofluorescein diacetate) (H<sub>2</sub>O<sub>2</sub> accumulation) were used to determine the nature of cell death. My results showed that there was no significant difference in necrosis or ROS accumulation between Wt and  $\Delta por1$  cells after treatment with Occidiofungin (Table 3.1). This suggests that Porin 1 is not required for the antifungal effects of Occidiofungin. The fact that Porin is not required for Occidiofungin to induce necrosis also argues against a role of a constitutive MAPK dependent

activation of the CWI pathway, that has been shown to drive necrosis upon Actin stabilisation (43). As *S. cerevisiae* cells possess two porin genes, *POR1* and *POR2* (50), it is possible that the second porin gene may provide redundancy and it may be necessary to generate a double knockout strain to rule out porin involvement altogether. However, deletion of *POR1* was sufficient to prevent Actin stabilisation induced necrosis (50).

To investigate whether Occidiofungin may function via an interaction with Actin, I made use of a library of *ACT1* mutant strains (45). The rationale for this experiment was that mutations in an Occidiofungin binding site may impart resistance to the drug, or that we may observe a synthetic interaction between the drug and Actin mutant strains. The majority of Actin mutant strains showed similar levels of inhibition by Occidiofungin, indicating a strong antifungal effect. However in one strain, expressing the *act1-III* allele, I observed no significant difference between the control and Occidiofungin treatment (Table 3.3). Interestingly this mutation has been shown to inhibit an interaction between Actin and the Actin nucleating protein Las17 (which is the yeast homologue of mammalian WASP), which forms Actin branches within cortical Actin patches and is crucial for endocytosis in yeast (51). This finding may suggest a putative Actin binding site for Occidiofungin; however I cannot rule out an indirect effect of *act1-III* expression that may influence for example, drug uptake or expulsion from cells. Further experimentation should address whether the slow growth observed in the *act1-III* mutant strain (or other indirect phenotypes effects associated with *act1-III* expression, such as cell wall thickness, membrane composition or expression of drug transporters) are responsible for Occidiofungin resistance. Further *ACT1* mutants could be also tested, for example cells expressing the *act1-104* allele (which lies directly adjacent to the *act1-III* mutation and also disrupts Las17 binding) could be tested for resistance to Occidiofungin (51). We might expect that the *act1-104* allele would also impart Occidiofungin resistance if the region of Actin between sub-domains III and IV (Figure 5.1 B) represents an Occidiofungin binding site.

As the *act-1-111* allele disrupts an interaction that is crucial for Actin patch mediated endocytosis we would expect that Occidiofungin would have a strong effect on this process if it does bind directly to Actin in cells. To investigate this I introduced an ABP1-GFP plasmid to *S.cerevisiae* cells to allow for real time visualisation of the cortical Actin patch dynamics using fluorescent microscopy (Figure 3.12). I hypothesised that Occidiofungin would inhibit the internalisation of cortical Actin patches if it bound to Actin and inhibited the Las17 binding to Actin that is crucial for endocytosis (52). However my experiment showed that even after 90 minutes of treatment with  $0.35\mu\text{g mL}^{-1}$  Occidiofungin, the endocytosis of the Actin cortical patches was unaffected. As endocytosis was not disrupted this therefore suggests that Las17 binding to Actin was not disrupted by Occidiofungin. A caveat to this finding is that the cells that I took timelapse images of after 90 minutes of treatment with Occidiofungin may have been viable, perhaps inherently resistant to the drug, and so displayed similar Actin cortical patch dynamics to untreated cells. Published data suggested that Occidiofungin treatment led to a depolarisation of Actin patches, which is a stress response that the Actin cytoskeleton displays, and that the Actin patches mediate CWI signalling and are not mobile or endocytosed (44). It may be the case that we would observe a similar depolarisation of Actin through treatment with Occidiofungin if we fixed cells and treated with rhodamine phalloidin as an F-Actin stain. The use of rhodamine phalloidin to analyse the Actin patches under a microscope in combination with PI staining, would allow me to ascertain whether a cells is beginning to show signs of necrosis. This would then give a good indication that the cell being visualised has been exposed to Occidiofungin. However as we did not observe evidence of porin mediated CWI activation it may also be the case that the published rhodamine phalloidin data is misleading. Further investigation is required to resolve this conflicting data.

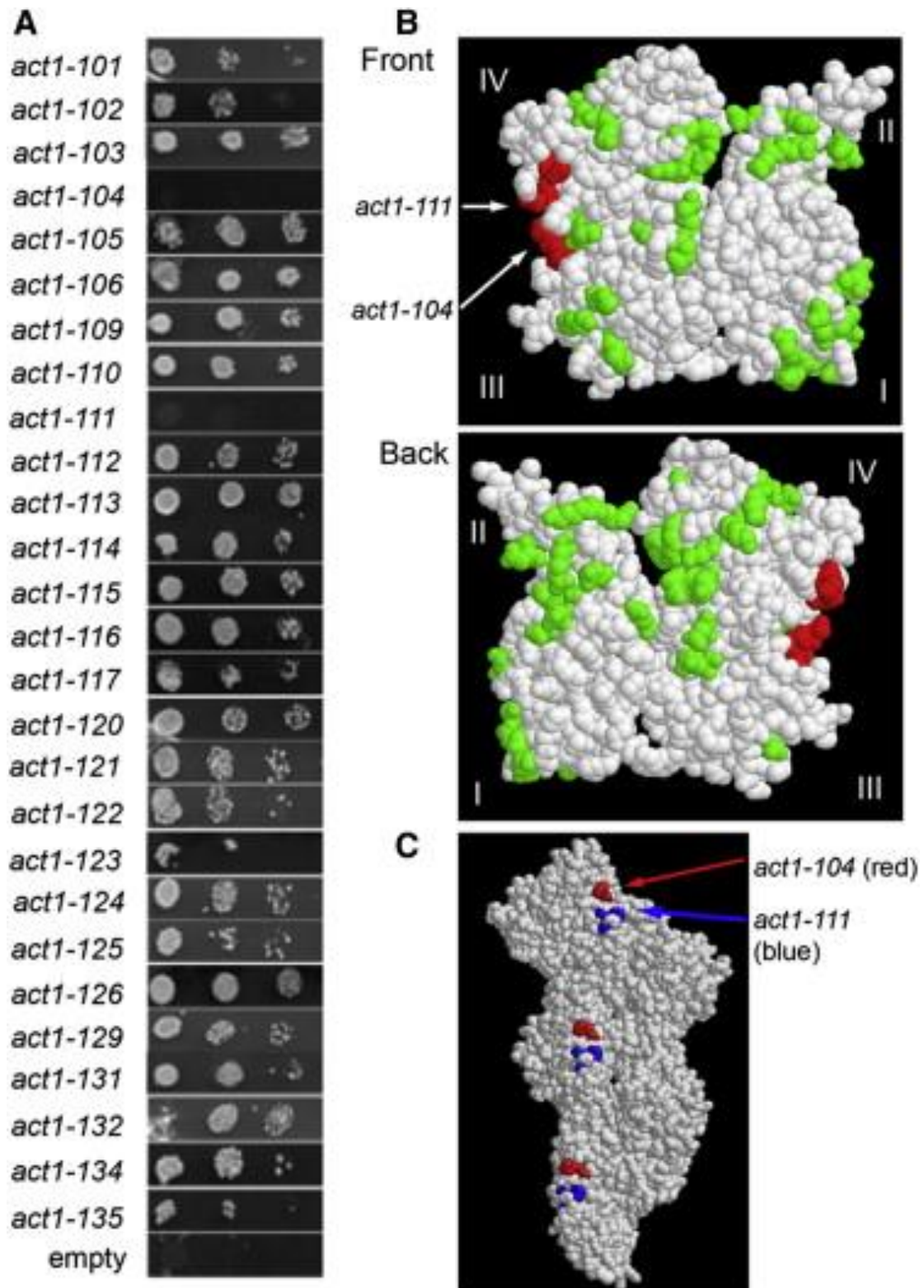


**Figure 5.1** Diagrams to demonstrate Las17 binding Actin. A - represents Yeast two-hybrid plasmids, where 27 Actin alleles were tested for binding to Las17, all but *act1-104* and *act1-111* interacted with Las17. B - Actin structure highlighting the 27 alleles, Las17 non-interacting alleles are in red. C - Filament model of Actin with *act1-104* residues in red and *act1-111* residues in blue (51)

My data clearly shows that Occidiofungin leads to cell death as a result of necrosis (Figure 3.6). It is possible that this may occur as a result of Actin stabilisation, however another possibility is that the drug directly induces membrane instability directly and independently of Actin. I was fortunate to be able to use Alkyne Occidiofungin, which is a fluorescent form of the drug. This experiment allowed me to visualise where Occidiofungin localised on a *Candida albicans* cell after treatment with  $0.4\mu\text{g mL}^{-1}$  Alkyne Occidiofungin for a total of 50 minutes. What the resulting images showed were that Alkyne Occidiofungin localised to the outside of the cell, close to or at the cell wall (Figure 3.19). This was determined by the use of Calcofluor White which stains chitin within the fungal cell wall. Alkyne Occidiofungin appeared to display this same localisation as the Calcofluor White stain (See Figure 3.19). There were no instances where the Alkyne Occidiofungin was observed within the cell, indicating that it does not become internalised as might be expected if it became imbedded within the plasma membrane and endocytosed. The lack of internalisation provides further indication that Occidiofungin does not bind Actin in living cells, however I cannot rule out the possibility that the Alkyne group alters the localisation and uptake of Occidiofungin. Interestingly the Alkyne Occidiofungin appeared to show a higher density at specific loci on the cell, if it were to target the cell wall this localised density could be attributed to chitin deposition, being excluded from areas of recent bud separation. There are limitations in the use of Alkyne Occidiofungin, one of the major ones being that Alkyne Occidiofungin has been shown to have an MIC that is eight times higher than Occidiofungin (53), this therefore could mean that Alkyne Occidiofungin is not present at a high enough concentration to elicit a damaging effect that would be more representative of Occidiofungin and therefore future experimentation could look into increasing the concentration of Alkyne Occidiofungin to assess whether this changes the localisation of the drug on the cell.

## ***4.2 Occidiofungin effects on lipid storage***

In my research I also explored the effect that Occidiofungin had on lipid droplet storage. As Porin 1 is essential for maintaining mitochondrial function and the mitochondria is crucial in regulating lipid metabolism we would expect that the  $\Delta por1$  *S.cerevisiae* cells to automatically display a lower percentage of lipid droplets when compared to the Wt. This percentage was 68.5% when the average number of lipid droplets per cell was compared to the Wt (Table 3.2). If Occidiofungin had Porin 1 as a downstream mediator in causing this cell necrosis, we may expect to see an increase in lipid droplet count in Wt cells that is lost upon porin deletion. However after Occidiofungin addition for 1 hour and 2 hour the % difference between the lipid droplet count in the Wt and  $\Delta por1$  cells was relatively unchanged and therefore it is logical to interpret that Porin 1 and lipid droplet formation are factors in the mode of action of Occidiofungin.

## ***4.3 Occidiofungin is a promising anti-fungal***

Current literature values for the MIC of Occidiofungin for *C. albicans*, *C. glabrata*, *C. tropicalis*, and *C. parapsilosis* were determined to be within a range of 2.0 to 0.5  $\mu\text{gml}^{-1}$  (57). A useful antifungal should display low toxicity and a broad spectrum of activity against fungal pathogens. In my experimentation Occidiofungin was able to inhibit the growth of *S.cerevisiae* cells by half ( $\text{MIC}_{50}$ ) at a concentration of 0.35  $\mu\text{gml}^{-1}$  and this was then used as a baseline for a majority of my experimentation (Figure 3.1). The  $\text{MIC}_{50}$  concentration was sufficient to induce necrosis in 80% of the cell population after 120 minutes indicating that it has a fungicidal effect (Figure 3.6). Additional experiments should monitor cell death over a longer period to determine whether the 20% of non-necrotic cells are inherently resistant to the drug. This has implications for the development of drug resistance. It would be important to determine

whether the resistance is heritable (genetic/epigenetic) or whether this represents a sub population of stress resistant cells within the wild type strain used. The variability of effects of the drug were observed in different species of pathogenic *Candida*. *Candida glabrata* (*N. glabratus*) was the most sensitive, being almost 100% necrotized in 90 minutes of treatment (See Figure 3.18). *Candida glabrata* is more closely related to *Saccharomyces cerevisiae* than to *Candida* species. In fact, *N. glabratus* belongs to the group of *Nakaseomyces* inside the whole genome duplication clade within *Saccharomycetaceae* (54). This data provided evidence that Occidiofungin is fungicidal to a range of pathogenic yeast but that each presents different sensitivity. It will be important to test larger panels of clinical isolates to ascertain the range of sensitivity. Potential clinical application to treat varying forms of fungal infection, we would need to employ these cell necrosis assays on a broader range of fungal pathogens, to determine how broad a range of activity Occidiofungin possesses, and therefore just how effective it could be as an antifungal.

*Candida albicans* readily forms biofilms and this is a clinical issue as such structures are highly resistant to antifungal treatment. To determine whether Occidiofungin could be used to treat biofilms I also conducted a Biofilm assay using XTT which measures the metabolic activity of cells within a biofilm. *C. albicans* biofilms were treated at 6.4 and 3.2  $\mu\text{g mL}^{-1}$  Occidiofungin at attachment and growth phases of biofilm maturation, whilst also having a control in which no drug was added at any stage. My results showed that Occidiofungin was effective at decreasing the metabolic activity of the biofilm when compared to the untreated control (See Figure 3.17). This highlighted that Occidiofungin has the potential to be used as a preventative measure in scenarios where biofilm formation is implicated, such as colonisation of medical implant devices. The application of Occidiofungin could be employed to prevent biofilm formation in such cases and improve patient healthcare. This assay does have its limitations however as biofilms are not solely made up of *Candida albicans* cells *in vivo*, they can be made up of an

amalgamation of different fungal and bacterial cells and this combination could potentially cause a resistance to the drug and allow the biofilms to mature. Therefore in order to assess this further it would be ideal to isolate yeast and bacteria that are present on medical implantation devices and grow them in unison allowing them to form a biofilm. The controls that were implemented in my experimentation can then be repeated and this would determine whether Occidiofungin is just as effective as it is in preventing *Candida albicans* growth within a mixed species biofilm.

This research also tested whether Occidiofungin displayed fungal specificity. As Occidiofungin appears to cause cell lysis we made use of a haemolysis assay, which employed the use of sheep blood. A 10% SDS positive control was used to demonstrate that red cell lysis could be observed and four different concentrations of Occidiofungin, representing 1/10x, 1x, 10x and 100x the MIC<sub>50</sub>, were used. We did not observe any red blood cell lysis from Occidiofungin up to the highest concentration of 35µgmL<sup>-1</sup> (See Figure 3.13). With this being a 100 fold increase from the MIC<sub>50</sub>, this suggests its effects on cell lysis are fungal specific. This finding also suggests that Occidiofungin does not target Actin in red blood cells as the cytoskeleton is essential for their integrity. A limitation of this assay is that the agar may prevent Occidiofungin action on red blood cells, to test this a liquid haemolysis assay could be conducted. Further assays could test blood from human participants.

Another experiment that was undertaken to assess toxicity was the use of *Galleria mellonella* as an infection model. This experiment tested whether Occidiofungin was toxic to a living eukaryotic animal. We also made use of *Galleria* to assess whether Occidiofungin treated cells were less virulent. My data showed that even at 100 fold concentration to the MIC<sub>50</sub> we did not observe significant toxicity to the larvae (See Figure 3.14). This provided further supporting evidence for Occidiofungin being fungal specific in its mode of action. I also conducted another survival assay, to assess whether Occidiofungin was able to inhibit and or treat *Candida*

*albicans* infection within the wax moth larvae. This employed a few key groups; *Candida* infected, *Candida* pre-treated with Occidiofungin and *Candida* infected alongside Occidiofungin injection. Interestingly the *Candida* and Occidiofungin co-injected animals (injected into opposite proleg) displayed the worst survival rate, with the entire population dead by day 4, as opposed to day 6 observed when *C. albicans* alone was injected (See Figure 3.15). It may be that the introduction of a second injection site could have caused an increased stress to the wax moth and this subsequently resulted in the faster health decline. However, injection of Occidiofungin into the animal at a distal site did not offer protection against *C. albicans* infection. This may suggest that the drug does not enter the *Galleria* haemolymph effectively to reach the site of infection. An additional experiment should co-inject Occidiofungin at the same pro-leg site to test this. The *Candida* Occidiofungin pre-treated control group however did display an increased survival rate when compared to *Candida* infected (See Figure 3.15). Here I observed that *Candida albicans* cells treated for 2 hours with Occidiofungin prior to injection, led to a 50% loss of viability by the 7<sup>th</sup> day as opposed to the 100% loss seen in the *Candida* infected control. This is consistent with Occidiofungin killing cells within a 2h period and a subsequent reduction in viable cell load. The significance of this is that if we can introduce Occidiofungin into a living system or area of infection, it has the potential application to slow the rate of infection. There are however limitations with the use of *Galleria mellonella* as an infection model, for example due to their simple immune system lacking complexity when compared to the mammalian immune system, this limits the ability to fully replicate the humane disease process and therefore to truly understand whether we would see the same effects within a human system, this is only applicable via testing on humans (55). Overall what these survivability assays show is that Occidiofungin has the ability to reduce the rate of infection and subsequent death toll on these wax moth larvae, if this reduced infection rate can

be seen within the mammalian system this could provide patients with a better chance at overcoming an infection via the slowing of the rate at which it occurs.

## **Conclusion**

My research indicates that Occidiofungin is fungicidal in action, leading to rapid necrosis, potentially by acting on the integrity of the cell wall and/or plasma membrane. Our data suggest that overall Actin dynamics may not be a primary driver of necrosis and cell death and that its binding may not represent a novel mechanism of action as has been suggested in the literature. Occidiofungin exhibits a broad range of activity against yeast species and against the biofilm mode of growth. Its necrotic effects are not carried through to higher eukaryotic and mammalian cells, suggesting a fungal specific mode of action. Further experiments are required to determine the mode of action that leads to necrosis, whether drug resistance can be acquired and whether Occidiofungin can act in synergy with existing antifungals. My results have clearly indicated the potency and broad spectrum activity that Occidiofungin possesses make it a good candidate as a future antifungal that can be employed to tackle infection as the threat of fungal disease increases.

## References

1. Puumala E, Fallah S, Robbins N, Cowen LE. Advancements and challenges in antifungal therapeutic development. *Clin Microbiol Rev.* 2024;37(1):e00142-23
2. Vicente F, Reyes F, Genilloud O. New Antifungal Drugs: Discovery and Therapeutic Potential. In: Deshmukh SK, Takahashi JA, Saxena S, editors. *Fungi Bioactive Metabolites*. Singapore: Springer; 2024.
3. Denning DW. Global incidence and mortality of severe fungal disease. *Lancet Infect Dis.* 2024;24(7):e428-e438.
4. Jafarlou M. Unveiling the menace: a thorough review of potential pandemic fungal disease. *Front Fungal Biol.* 2024;5.
5. Seyedmousavi S, Bosco S, de MG, de Hoog S, Ebel F, Elad D, et al. Fungal infections in animals: A patchwork of different situations. *Med Mycol.* 2018;56(Suppl 1):S165-S187.
6. Jabra-Rizk MA, Kong EF, Tsui C, Nguyen MH, Clancy CJ, Fidel PL Jr, et al. *Candida albicans* pathogenesis: fitting within the host-microbe damage response framework. *Infect Immun.* 2016;84(10):2724-39.
7. Parambath S, Dao A, Kim HY, Zawahir S, Alastruey Izquierdo A, Tacconelli E, Govender N, Oladele R, Colombo A, Sorrell T, Ramon-Pardo P, Fusire T, Gigante V, Sati H, Morrissey CO, Alffenaar JW, Beardsley J. Characteristics and global impact of invasive infections caused by *Candida albicans*: a systematic review. *FEMS Pathogens and Disease.* 2024.
8. Dadar M, Tiwari R, Karthik K, Chakraborty S, Shahali Y, Dhama K. *Candida albicans*—biology, molecular characterization, pathogenicity, and advances in diagnosis and control—an update. *Microb Pathog.* 2018;117:128-38.

9. Pappas PG, Lionakis MS, Arendrup MC, Ostrosky-Zeichner L, Kullberg BJ. Invasive candidiasis. *Nat Rev Dis Primers*. 2018;4:18026.
10. Andes DR, Safdar N, Baddley JW, Alexander BD, Brumble LM, Freifeld A, et al. The epidemiology and outcomes of invasive *Candida* infections among organ transplant recipients in the United States: results of the Transplant-Associated Infection Surveillance Network (TRANSNET). *Transpl Infect Dis*. 2016;18(6):921-31.
11. Drummond RA. *Candida albicans*. *BiteSized Immunology: Pathogens & Disease*. British Society for Immunology.
12. Carolus H, Van Dyck K, Van Dijck P. *Candida albicans* and *Staphylococcus* Species: A Threatening Twosome. *Front Microbiol*. 2019 Sep 17;10:2162.
13. World Health Organization. WHO fungal priority pathogens list to guide research, development and public health action report. October 2022.
14. Sikora A, Hashmi MF, Zahra F. *Candida auris*. [Updated 2023 Aug 28]. In: StatPearls [Internet]. Treasure Island (FL): StatPearls Publishing; 2024 Jan.
15. Biswal M, Rudramurthy SM, Jain N, Shamanth AS, Sharma D, Jain K, Yaddanapudi LN, Chakrabarti A. Controlling a possible outbreak of *Candida auris* infection: lessons learnt from multiple interventions. *J Hosp Infect*. 2017 Dec;97(4):363-70.
16. Fisher MC, Alastruey-Izquierdo A, Berman J, Bicanic T, Bignell EM, Bowyer P, et al. Tackling the emerging threat of antifungal resistance to human health. *Nat Rev Micro*. 2022;20(9):557-71.
17. Ghannoum MA, Rice LB. Antifungal agents: mode of action, mechanisms of resistance, and correlation of these mechanisms with bacterial resistance. *Clin Microbiol Rev*. 1999;12(4):501-517. doi: 10.1128/CMR.12.4.501.

18. Gray KC, Palacios DS, Dailey I, Endo MM, Uno BE, Wilcock BC, Burke MD. Amphotericin primarily kills yeast by simply binding ergosterol. *Proc Natl Acad Sci U S A*. 2012;109(7):2234-2239. doi: 10.1073/pnas.1117280109.
19. Denning DW. Echinocandin antifungal drugs. *Lancet*. 2003;362(9390):1142-1151. doi: 10.1016/S0140-6736(03)14472-8.
20. Ryder NS. Terbinafine: mode of action and properties of the squalene epoxidase inhibition. *Br J Dermatol*. 1992;126(Suppl 39):2-7. doi: 10.1111/j.1365-2133.1992.tb00001.x.
21. Vermes A, Guchelaar HJ, Dankert J. Flucytosine: a review of its pharmacology, clinical indications, pharmacokinetics, toxicity and drug interactions. *J Antimicrob Chemother*. 2000;46(2):171-179. doi: 10.1093/jac/46.2.171.
22. Chow EWL, Pang LM, Wang Y. From Jekyll to Hyde: The Yeast-Hyphal Transition of *Candida albicans*. *Pathogens*. 2021;10(7):859.
23. Brown AJP, Budge S, Kaloriti D, Tillmann A, Jacobsen MD, Yin Z, et al. Stress adaptation in a pathogenic fungus. *J Exp Biol*. 2014;217(1):144-55.
24. Kumar D, Kumar A. Molecular Determinants Involved in *Candida albicans* Biofilm Formation and Regulation. *Mol Biotechnol*. 2024;66:1640-1659.
25. Nobile CJ, Mitchell AP. Regulation of cell-surface genes and biofilm formation by the *C. albicans* transcription factor Bcr1p. *Curr Biol*. 2005;15(12):1150-5.
26. Nobile CJ, Andes DR, Nett JE, Smith FJ, Yue F, Phan QT, et al. Critical role of Bcr1-dependent adhesins in *C. albicans* biofilm formation in vitro and in vivo. *PLoS Pathog*. 2006;2(7):e63.
27. Nobile CJ, Fox EP, Nett JE, Sorrells TR, Mitrovich QM, Hernday AD, et al. A recently evolved transcriptional network controls biofilm development in *Candida albicans*. *Cell*. 2012;148(1-2):126-38.

28. Fox EP, Nobile CJ. A sticky situation: Untangling the transcriptional network controlling biofilm development in *Candida albicans*. *Transcription*. 2012;3(6):315-22.
29. Finkel JS, Mitchell AP. Genetic control of *Candida albicans* biofilm development. *Nat Rev Microbiol*. 2011;9(2):109-18.
30. Murillo LA, Newport G, Lan CY, Habelitz S, Dungan J, Agabian NM. Genome-wide transcription profiling of the early phase of biofilm formation by *Candida albicans*. *Eukaryot Cell*. 2005;4(9):1562-73.
31. Banerjee M, Uppuluri P, Zhao XR, Carlisle PL, Vipulanandan G, Villar CC, et al. Expression of UME6, a filament-specific regulator of *Candida albicans*, enhances biofilm formation and virulence. *Infect Immun*. 2013;81(9):3429-41.
32. Cavaleiro M, Teixeira MC. *Candida* Biofilms: Threats, Challenges, and Promising Strategies. *Front Med (Lausanne)*. 2018;5:28.
33. Gu G, Smith L, Liu A, Lu S. Genetic and Biochemical Map for the Biosynthesis of Occidiofungin, an Antifungal Produced by *Burkholderia contaminans* Strain MS14. *Appl Environ Microbiol*. 2011;77(17):6189-98.
34. Hansanant N, Smith L. Occidiofungin: Actin Binding as a Novel Mechanism of Action in an Antifungal Agent. *Antibiotics*. 2022;11(9):1143. doi:10.3390/antibiotics11091143.
35. Mithilesh Mishra, Junqi Huang, Mohan K. Balasubramanian, The yeast actin cytoskeleton, *FEMS Microbiology Reviews*, Volume 38, Issue 2, March 2014, Pages 213–227
36. Galletta BJ, Chuang DY, Cooper JA. Distinct Roles for Arp2/3 Regulators in Actin Assembly and Endocytosis. *PLoS Biol*. 2008;6(1):e1.

37. Newpher TM, Smith RP, Lemmon V, Lemmon SK. In Vivo Dynamics of Clathrin and Its Adaptor-Dependent Recruitment to the Actin-Based Endocytic Machinery in Yeast. *Dev Cell*. 2005;9(1):87-98
38. Mullins RD, Heuser JA, Pollard TD. The interaction of Arp2/3 complex with actin: nucleation, high affinity pointed end capping, and formation of branching networks of filaments. *Proc Natl Acad Sci U S A*. 1998;95(11):6181-6.
39. Pollard TD, Blanchoin L, Mullins RD. Molecular mechanisms controlling actin filament dynamics in nonmuscle cells. *Annu Rev Biophys Biomol Struct*. 2000;29:545-76.
40. Pollard TD, Borisy GG. Cellular motility driven by assembly and disassembly of actin filaments. *Cell*. 2003;112(4):453-65.
41. Sun Y, Martin AC, Drubin DG. Endocytic internalization in budding yeast requires coordinated actin nucleation and myosin motor activity. *Dev Cell*. 2006;11(1):33-46.
42. Smethurst DGJ, Dawes IW, Gourlay CW. Actin – a biosensor that determines cell fate in yeasts. *FEMS Yeast Res*. 2014 Feb;14(1):89-95.
43. Davis J, Meyer T, Smolnig M, Smethurst DGJ, Neuhaus L, Heyden J, Broeskamp F, Edrich ESM, Knittelfelder O, Kolb D, Haar TV, Gourlay CW, Rockenfeller P. A dynamic actin cytoskeleton is required to prevent constitutive VDAC-dependent MAPK signalling and aberrant lipid homeostasis. *iScience*. 2023 Aug 2;26(9):107539. doi: 10.1016/j.isci.2023.107539. PMID: 37636069; PMCID: PMC10450525.
44. Ravichandran A, Geng M, Hull KG, Li J, Romo D, Lu SE, Albee A, Nutter C, Gordon DM, Ghannoum MA, Lockless SW, Smith L. A Novel Actin Binding Drug with *In Vivo* Efficacy. *Antimicrob Agents Chemother*.
45. Johanna L Whitacre, Dana A Davis, Kurt A Toenjes, Sharon M Brower, Alison E M Adams, Generation of an Isogenic Collection of Yeast Actin Mutants and

Identification of Three Interrelated Phenotypes, *Genetics*, Volume 157, Issue 2, 1  
February 2001, Pages 533–543

46. Homann OR, Dea J, Noble SM, Johnson AD. A phenotypic profile of the *Candida albicans* regulatory network. *PLoS Genet.* 2009 Dec;5(12):e1000783. doi: 10.1371/journal.pgen.1000783. Epub 2009 Dec 24. PMID: 20041210; PMCID: PMC2790342.
47. Duvenage L, Pentland DR, Munro CA, Gourlay CW. An analysis of respiratory function and mitochondrial morphology in *Candida albicans*. *bioRxiv.* 2019 Jan 1;697516. doi: 10.1101/697516.
48. Whitacre J, Davis D, Toenjes K, Brower S, Adams A. Generation of an isogenic collection of yeast actin mutants and identification of three interrelated phenotypes. *Genetics.* 2001 Feb;157(2):533-43. doi: 10.1093/genetics/157.2.533. PMID: 11156976; PMCID: PMC1461522.
49. Pereira MF, Rossi CC, da Silva GC, Rosa JN, Bazzolli DMS. *Galleria mellonella* as an infection model: an in-depth look at why it works and practical considerations for successful application. *Pathog Dis.* 2020 Nov 11;78(8):ftaa056. doi: 10.1093/femspd/ftaa056. PMID: 32960263.
50. Strogolova V, Orlova M, Shevade A, Kuchin S. Mitochondrial porin Por1 and its homolog Por2 contribute to the positive control of Snf1 protein kinase in *Saccharomyces cerevisiae*. *Eukaryot Cell.* 2012 Dec;11(12):1568-72. doi: 10.1128/EC.00127-12. Epub 2012 Oct 26. PMID: 23104570; PMCID: PMC3536279.
51. Urbanek AN, Smith AP, Allwood EG, Booth WI, Ayscough KR. A novel actin-binding motif in Las17/WASP nucleates actin filaments independently of Arp2/3. *Curr Biol.* 2013 Feb 4;23(3):196-203. doi: 10.1016/j.cub.2012.12.024.

52. Naqvi SN, Zahn R, Mitchell DA, Stevenson BJ, Munn AL. The WASp homologue Las17p functions with the WIP homologue End5p/verprolin and is essential for endocytosis in yeast. *Curr Biol.* 1998 Aug 27;8(17):959-62. doi: 10.1016/s0960-9822(98)70396-3. PMID: 9742397.
53. Williams DE, Dalisay DS, Wang P, Centko R, Chen J, Andersen RJ. Occidiofungin, a unique antifungal glycopeptide produced by a strain of *Burkholderia contaminans*. *J Nat Prod.* 2012;75(4):641-644. doi: 10.1021/np200973r.
54. Gabaldón T, Martin T, Marcet-Houben M, Durrens P, Bolotin-Fukuhara M, Lespinet O, et al. Comparative genomics of emerging pathogens in the *N. glabratus* clade. *BMC Genomics.* 2013 Sep 14;14(1):623. doi: 10.1186/1471-2164-14-623. PMID: 24034898; PMCID: PMC3847288.
55. Tsai CJ, Loh JMS, Proft T. *Galleria mellonella* infection models for the study of bacterial diseases and for antimicrobial drug testing. *Pathogens.* 2020 Aug;9(8):620. doi: 10.3390/pathogens9080620.
56. <https://www.sigmaaldrich.com/deepweb/assets/sigmaaldrich/product/documents/357/638/11465015001.pdf>
57. Ellis D, Gosai J, Emrick C, Heintz R, Romans L, Gordon D, Lu SE, Austin F, Smith L. Occidiofungin's chemical stability and in vitro potency against *Candida* species. *Antimicrob Agents Chemother.* 2012 Feb;56(2):765-9. doi: 10.1128/AAC.05231-11. Epub 2011 Nov 21. PMID: 22106210; PMCID: PMC3264235.